Targeting gastric cancer stem-like cells by modulating mitochondrial redox homeostasis

Hae-Ji Choi

Department of Medical Science

The Graduate School, Yonsei University

Targeting gastric cancer stem-like cells by modulating mitochondrial redox homeostasis

Hae-Ji Choi

Department of Medical Science

The Graduate School, Yonsei University

Targeting gastric cancer stem-like cells by modulating mitochondrial redox homeostasis

Directed by Professor Jae-Ho Cheong

The Doctoral Dissertation
submitted to the Department of Medical Science,
the Graduate School of Yonsei University
in partial fulfillment of the requirements for the degree
of Doctor of Philosophy of Medical Science

Hae-Ji Choi

June 2020

This certifies that the Doctoral Dissertation of Hae-Ji Choi is approved.

Thesis Supervisor: Jae-Ho Cheong

Thesis Committee Member#1: Ho-Geun Yoon

Thesis Committee Member#2: Sang Won Kang

Thesis Committee Member#3: Soo Han Bae

Thesis Committee Member#4: Ji-Hwan Ryu

The Graduate School
Yonsei University

June 2020

ACKNOWLEDGEMENTS

I sincerely appreciate all those who gave me emotional support as well as valuable advice during my doctoral degree course.

Firstly, I deeply appreciate my supervisor professor Jae-Ho Cheong for excellent guidance during my doctoral degree course. This thesis would not have been possible without his continuous support, warm personality, and remarkable patience. It was honor to study in his laboratory.

I appreciate the members of my dissertation committee, professor Ho-Geun Yoon, Sang Won Kang, Soo Han Bae and Ji-Hwan Ryu for inspiring suggestions and criticisms.

I would like to express my sincere gratitude to my lab members, Yoo-Lim Jhe, Jungmin Kim, Ju Yeon Lim and Jae Eun Lee. I truly thank Hyun Jung Kee and Ki Cheong Park for advising my research as well.

Also thank my friends, Ara, Ji Hye and Ji Eun for their support and warmhearted words.

Hae-Ji Choi

TABLE OF CONTENTS

.

LIST OF FIGURES

LIST OF TABLES

ABSTRACT

Targeting gastric cancer stem-like cells by modulating mitochondrial redox homeostasis

Hae-Ji Choi

Department of Medicine or Medical Science
The Graduate School, Yonsei University

(Directed by Professor Jae-Ho Cheong)

Increased oxidative phosphorylation (OXPHOS) and reactive oxygen species (ROS) levels are inherently linked. ROS are essential signaling molecules, with detrimental effects when produced in excess during chemotherapy, leading to cell death. Cancer stem-like cells (CSCs) are subpopulation of tumor cells resistant to chemotherapy, highly invasive and metastatic, driving malignant cancer behavior. In this study, we demonstrated that CSCs exhibit increased OXPHOS but paradoxically low ROS levels. Considering the detrimental effects of large amounts of ROS, CSCs have developed potential mechanisms for quenching excess ROS to maintain redox homeostasis. We aimed to investigate the distinct metabolic features and mechanisms of ROS regulation in gastric CSCs and explore potential therapeutic strategies targeting CSCs.

Human gastric cancer cell lines, AGS and MKN1, were subjected to liquid chromatography/mass spectrometry-based metabolomic and microarray analyses. Mitochondrial properties such as mitochondrial mass, membrane potential, and ROS were assessed by flow cytometry analysis. CSCs with increased OXPHOS levels maintained low ROS levels by coupling FoxM1-dependent Prx3 expression and fatty acid oxidation-mediated NADPH regeneration. Thus, interventions targeting ROS homeostasis in CSCs may be a useful strategy for targeting this drug-resistant tumor cell subpopulation.

Key words: oxidative phosphorylation; reactive oxygen species; cancer stem-like cell; FoxM1; fatty acid oxidation

Targeting gastric cancer stem-like cells by modulating mitochondrial redox homeostasis

Hae-Ji Choi

Department of Medicine or Medical Science
The Graduate School, Yonsei University

(Directed by Professor Jae-Ho Cheong)

I. INTRODUCTION

Adenosine triphosphate (ATP) is the main source of energy for most cellular processes. ATP can be produced by distinct cellular processes; the two main pathways in eukaryotes are (1) glycolysis and (2) oxidative phosphorylation (OXPHOS).

In 1924, Otto Warburg observed that cancer cells tend to metabolize most glucose to lactate regardless of whether adequate oxygen is present (aerobic glycolysis) [1,2].

This implies that cancer cells preferentially produce ATP via glycolysis, even in the presence of oxygen [3]. Although ATP generation by glycolysis can be more rapid than by OXPHOS, the metabolism of glucose to lactate generates

only 2 ATPs per molecule of glucose, whereas OXPHOS generates up to 36 ATPs per molecule of glucose consumed [2]. This shift therefore demands that cancer cells conduct an abnormally high rate of glucose uptake to secure their increased energy, biosynthesis and redox needs. Mitochondrial OXPHOS has recently gained much attention, in part because of cancer stem cells. The existence of a relatively rare, highly drug resistant, quiescent or slow-proliferating population of tumor-driving cells termed cancer stem cells (CSCs). The metabolic phenotype of CSCs appears to vary across tumor types. While in breast cancer [4] and nasopharyngeal carcinoma CSCs [5] were found to be predominantly glycolytic, CSCs in glioma and glioblastoma [6,7], lung cancer [8], leukemia [9-11] and pancreatic cancer [3] appear to rely on mitochondrial OXPHOS. Furthermore, the inhibition of mitochondrial OXPHOS could result in reversing the drug resistance in various preclinical cancer models [12].

In eukaryotes, OXPHOS takes place inside mitochondria. Mitochondria are bioenergetics and biosynthetic organelles. The tricarboxylic acid (TCA) cycle uses substrates from glycolysis, fatty acid oxidation, and amino acid catabolism to generate building blocks and high-energy electrons (NADH and $FADH_2$) to power the electron transport chain (ETC) [13].

Under normal conditions, mitochondria trigger redox signaling through the release of reactive oxygen species (ROS) from the ETC [14].

Redox is a balance of the reduced state versus the oxidized state of a biochemical system. This balance is influenced by the level of ROS. The

regulation of redox homeostasis is fundamental to maintaining normal cellular functions and ensuring cell survival [15].

ROS are by-products of aerobic metabolism with unpaired electrons derived from incomplete reduction of oxygen that are perpetually generated, transformed and eliminated in a variety of cellular processes including metabolism, proliferation, differentiation, immune system regulation and vascular remodeling [16]. ROS is a collective term that includes the superoxide anion (O_2^-), hydrogen peroxide (H_2O_2) and hydroxyl radical (•OH) [17].
Mitochondria are an important source of ROS within most mammalian cells [18-22]. During normal cellular respiration in aerobic organisms, electrons are passed through a series of mitochondrial complexes to the terminal electron acceptor, molecular oxygen. Complex I and Complex III of the ETC are the major sites for ROS production[23-25].

Mammalian complex I is the entrance of electrons from NADH and is ~1 MDa complex comprising 45 polypeptides [26,27]. An FMN cofactor accepts electrons from NADH and passes through a chain of seven FeS (iron-sulfur) centers to the CoQ reduction site [26,27]. Therefore, oxygen has a chance to react with electron at reduced FMN and CoQ reduction site rather than FeS which locates in the water-soluble arm of complex I [28].

Leakage of electrons from Complex III, primarily in reactions mediated by Coenzyme Q which is an essential carrier for the electron transfer in the mitochondrial respiratory chain for ATP production. Coenzyme Q exists in the

oxidized (ubiquinone), partially reduced (ubisemiquinone radical) and in the reduced form (ubiquinol). Q cycle is a chain of processes where electrons flow from ubiquinol to cytochrome c at complex III. In this reaction, ubisemiquinone radical can react with oxygen to form superoxide [28-30].

There is an important role for ROS to maintain functions of stem cells, cancer cells and cancer stem cells. Owing to various stem cells reside in a hypoxic niche, hypoxia contributes to the maintenance of stem cells. Hypoxia-inducible factorα (HIF1α) promotes glycolysis and thereby stem cells must rely on anaerobic glycolysis, rather than mitochondrial OXPHOS, to support ATP production [18,31,32]

To maintain stemness, stem cells must minimize ROS damage-it has been suggested that a 'ROS rheostat' monitors stem cell fate decisions with regard to self-renewal or commitment [20,21,33-36]. The low ROS concentrations that seem to be critical for self-renewal of haematopoietic stem cells (HSCs)[35,37] are also a property of mammary epithelial stem cells [38,39].

Unlike stem cells, cancer cells are characterized by increased aerobic glycolysis and high levels of oxidative stress [40]. This oxidative stress is exerted by ROS that accumulate as a result of an imbalance between ROS generation and elimination, and this has been implicated in carcinogenesis [22], neurodegeneration [23], atherosclerosis [24], diabetes [25], and aging [26]. The high levels of ROS in cancer cells are a consequence of alterations in several signaling pathways that affect cellular metabolism [14]. The ROS levels are

reduced by elevated antioxidant defense mechanisms in cancer cells [41].

Scavenging of ROS is mediated by a set of 'antioxidant' enzymes that are expressed in various subcellular compartments [14]. Superoxide dismutases (SODs) are expressed in various cellular compartments and rapidly convert O_2^- into H_2O_2 [27]. To counter the effects of H_2O_2, peroxiredoxins (PRXs), glutathione peroxidases (GPXs), and catalase (CAT) convert intracellular H_2O_2 into water [17].

Although cancer stem cells share similar phenotypes with normal stem cells such as self-renewal, relatively little is known about their redox status [15]. A recent study has shown that breast and liver cancer stem cells tend to have lower concentrations of ROS than non-tumorigenic cells owing to the increased expression of ROS-scavenging systems [41,42]. Heterogeneity of ROS levels may influence the extent to which CSC-enriched populations are resistant to therapies such as ionizing radiation [41].

Pancreatic cancer stem cells also showed that low MYC expression in human CSCs allowed high PGC1A expression levels, which resulted in enhanced mitochondrial biogenesis, strong mitochondrial activity and antioxidant properties, and subsequently low mitochondrial ROS levels, as a prerequisite for their stemness function [3].

Colon cancer stem cells demonstrated that highly expressed mitochondrial antioxidant Prx3 plays a critical role in maintaining mitochondrial function via elimination of ROS produced by ATP production in the OXPHOS system in

CSCs [43].

Breast cancer stem cells suggested another features of CSCs that the snail-G9a-Dnmt1 complex repressed FBP1 expression in basal-like breast cancer; this results in increased CSC-like characteristics and tumorigenicity by enhancing aerobic glycolysis and by suppression of ROS production [4].

NADPH locates separately in cytosolic and mitochondrial pools providing reducing power in each respective location [44]. There are multiple NADPH producing pathways in the mammalian cells [45].

Concurrent with these previous findings, we recently reported that highly metastagenic and drug-resistant subpopulations of tumor cells exhibit a distinct form of energy metabolism that does not rely on glycolysis but rather depends on mitochondria-centric metabolism[46-48]. Since increased OXPHOS and reactive oxygen species (ROS) levels are inherently linked, highly malignant subpopulations of cancer cells are expected to have elevated ROS levels[49]. However, ROS production beyond the physiological range can be detrimental, even to cancer cells.

The efficacy of many anticancer therapeutics including chemotherapy and ionizing radiation is based on their ability to increase ROS levels in tumor cells. However, it is currently unclear how most malignant cancer cells can depend on the OXPHOS-prone metabolic phenotype while maintaining disproportionately low levels of ROS. We hypothesized that maintenance of low ROS levels is one of the mechanisms of drug resistance in CSCs. To test this hypothesis, we investigated the distinct metabolic features and mechanisms of ROS regulation in

CSCs, selected from gastric cancer cell lines, to explore the potential of therapeutic strategies targeting CSCs.

II. MATERIALS AND METHODS

1. Cell culture conditions

The human gastric cancer cell lines, AGS and MKN1, were obtained from the Korean Cell line Bank (Seoul, Korea) and grown in RPMI-1640 medium with 10% fetal bovine serum in a humidified incubator containing 5% CO2 at 37 ℃. Stem-like cancer cells (S-cells) were generated by in-vitro chronic metabolic stress culture, as described previously [46].

2. Intracellular metabolite extraction

Parental cells (P-cells) and S-cells were plated in presence of 5.5 mM [$^{13}C_6$] glucose and 100 μM [$^{13}C_{16}$] palmitate (Cambridge Isotope Labs, Tewksbury, MA, USA) for 48 hours. The cells were washed twice with ice-cold PBS, and intracellular metabolites were extracted with a cold solution of methanol, acetonitrile, and water (5:3:2). The cell extracts were centrifuged at 16,000 ×g for 10 minutes at 4℃, and the supernatants were assessed via LC-MS analysis.

3. LC-MS-based metabolomics

LC-MS analysis was performed as described previously [50].

4. Microarray analysis

The NuRNA^{TM} Human Central Metabolism PCR Array (Arraystar, Inc., Rockville, MD, USA) was used to identify mRNA transcripts with differential expression between P-cells and S-cells. The array covers 373 transcripts encoding enzymes or proteins involved in cell metabolism. Samples were used for array analysis in accordance with the manufacturer's protocol and each analysis was performed in triplicate.

5. Fluorescence-activated cell sorting (FACS) and flow cytometry

Human gastric cancer cells (AGS and MKN1) were dissociated into single cells, washed with PBS, and stained with fluorescent antibodies for CD133-PE (BD Biosciences, Franklin Lakes, New Jersey) and CD44-FITC (BD Biosciences, Franklin Lakes, New Jersey). To determine the effect of ROS levels on M-and E-BCSCs in breast cancer cell lines, MCF7 were incubated with antibodies against CD24-PE (BD Biosciences, Franklin Lakes, New Jersey) and CD44-FITC. Content of ALDH $^{+}$ E-BCSCs was determined by Aldefluor assay (StemCell Technologies) per manufacturer`s instructions. After labeling, cells were sorted using a BD FACSAria flow cytometer (BD Biosciences, Franklin Lakes, NJ, USA).

6. Western blot analysis

Cells were lysed in lysis buffer (50 mM Tris-HCl, pH 7.4, 150 mM NaCl, 1 mM EDTA, and 1% Triton-X100) containing 1× protease

inhibitor cocktail (Sigma, St. Louis, MO, USA) and 1× phenylmethylsulfonyl fluoride (Sigma). Protein concentration was quantified using a BCA protein concentration assay kit (Thermo Fisher Scientific, Waltham, MA, USA). Equal amounts of protein were electrophoresed on sodium dodecyl sulfate-polyacrylamide gels and transferred onto polyvinylidene difluoride membranes. The membranes were incubated with primary antibodies in 2% skim milk containing 0.05% Tween-20 overnight at 4℃. The membranes were incubated with horseradish peroxidase-conjugated secondary antibody for 1 h at room temperature and visualized by electrochemiluminescence (Thermo Fisher Scientific).

7. Reverse transcription-quantitative PCR

Total RNA was isolated with TRIzol (Invitrogen, Carlsbad, CA, USA), and 1 μg of total RNA was used for cDNA synthesis using M-MLV reverse transcriptase (Mbiotech, Hanam-si, Korea). Quantitative PCR was carried out using SYBR Green PCR Master Mix (PhileKorea, Seoul, Korea). Experimental cycle threshold values were normalized to that of *GAPDH*, and relative mRNA expression was calculated versus *GAPDH* expression.

8. Lactate production

A lactate assay kit (Biovision Research Products, Milpitas, CA, USA) was used to measure extracellular lactate following the manufacturer's instructions. Briefly, equal numbers of cells were seeded into 6-well plates and cultured in serum-free media for 24 hours. The culture medium was then mixed with the reaction solution. Lactate levels were measured at 570 nm using a microplate reader. The cells were trypsinized, and cell number was counted using trypan blue. Absorbance values were normalized to the cell number.

9. Membrane potential assay

Mitochondrial membrane potential was measured using JC-1 dye (Invitrogen) according to the manufacturer's instructions. Briefly, equal numbers of cells were seeded into 6-well plates; after 72 hours, 2 μM JC-1 was added and the cells were incubated at 37 ℃ for 15 min. Carbonyl cyanide chlorophenylhydrazone (CCCP; Sigma) was used as a control to confirm that the JC-1 response was sensitive to changes in membrane potential. The cells were then trypsinized and washed twice with PBS, after which fluorescence was analyzed using a BD FACS LSRII flow cytometer.

10. Intracellular ROS

To measure intracellular ROS levels, 10 μM DCF-DA (Sigma) was used as a fluorescent dye. The cells were stained with DCF-DA for 30

min at 37℃, trypsinized, washed thrice with PBS, and immediately analyzed with a BD FACS LSRII flow cytometer.

Mitochondrial ROS levels were assessed using a MitoSOX RED mitochondrial superoxide indicator (Thermo Fisher Scientific) in accordance with the manufacturer's protocol. The MitoSOX RED reagent is a live-cell permeant that is rapidly and selectively targeted to the mitochondria. The parental or cancer stem-like cells were incubated with MitoSOX reagent for 10 minutes at 37℃ while protected from light. After the cells were washed thrice with PBS, they were collected, and MitoSOX red signal was detected by flow cytometry. ROS production was visualized in cells loaded with 10 μM DCF-DA (Sigma) for 30 minutes at room temperature. ROS-induced green fluorescence of DCF was imaged using 488-nm laser excitation. The laser power was set to 1–3%.

11. Oxygen consumption rate

The oxygen consumption rate was measured using an optical fluorescent oxygen sensor in a Seahorse Bioscience XF96 Extracellular Flux Analyzer (North Billerica, MA, USA). Briefly, the cells were seeded in quadruplicate at equal densities in XF96 culture plates. Cell media were changed, after 24 hours of cell seeding, to unbuffered Dulbecco's modified Eagle's medium, in accordance with the manufacturer's protocol. Oxygen consumption was measured with sequential injection of oligomycin, FCCP, and rotenone/antimycin A.

12. Glucose uptake and mitochondrial mass

Cells were incubated for 30 minutes at 37°C with 100 μM 2-*N*-(7-nitrobenz-2-oxa-1,3-diazol-4-yl)amino)-2-deoxyglucose (2-NBDG) and 100 nM Mitotracker Deep Red FM (both from Life Technologies, Carlsbad, CA, USA) prior to FACS analysis.

13. $NADP^+$/NADPH ratio determination

Colorimetric analysis of the cell lysates was performed using the NADP/NADPH Quantitation Kit (Biovision Research Products) in accordance with the manufacturer's instructions.

14. Quantification and statistical analysis

The overall survival data obtained from patients with gastric, breast, lung, and ovarian cancer were analyzed by the Kaplan-Meier Plotter (http://kmplot.com/analysis). Statistics was determined by paired Student's t test and ANOVA using GraphPad Prism 7 software (GraphPad, Inc., La Jolla, CA, USA). Results are presented as the mean ± standard deviation for representative experiments with 2–3 independent biological repeats. A P-value < 0.05 was considered statistically significant.

Table 1. Primer used for quantitative real time PCR (qRT-PCR)

GENE	FORWARD PRIMER	REVERSE PRIMER
FOXM1	GGAGGAAATGCCACACTTAGC	TGTAGGACTTCTTGGGTCTTGG
CATALASE	GATAGCCTTCGACCCAAGCA	ATGGCGGTGAGTGTCAGGAT
GLRX5	AGCTCCGACAAGGCATTAAA	AGTGGATCCCCAGCTTTTTC
GPX1	CCCTCTGAGGCACCACGGT	TAAGCGCGGTGGCGTCGT
GPX4	GCCTTCCCGTGTAACCAGT	GCGAACTCTTTGATCTCTTCGT
GSTK1	TCCAGATTCCCATCCACTTC	GACGCTTTCTCCAGCATCTC
GSTM1	CTATGATGTCCTTGACCTCCACCGTATA	ATGTTCACGAAGGATAGTGGGTAGCTGA
GSTM4	TTGGAGAACCAGGCTATGGAC	TTCCCCAGGAACTGTGAGAAGT
MGST2	CTGCTGGCTGCTGTCTCTATTC	TTGTTGTGCCCGAAATACTCTC
PRDX 1	CGGGCCTCTAGATCACTTCT	TATGTCTTCAGGAAATGCTA
PRDX 2	TTCAAGCTTATGGCCTTCCG	TCTAGACTAATTGTGTTTGG
PRDX 3	GTTGTCGCAGTCTCAGTGGA	GACGCTCAAATGCTTGATGA
PRDX 4	CGCTGGCTTGGAAATCTTCG	GCTTCTGCTGCCGCTACTG
PRDX 5	ATCAGCCAGGAGCCGAACC	GTCCGCAGTTTCAGCAGAGC
PRDX 6	GGCAAGATGGTCCTCAACAC	GGGAGACTCATGGGGCATTC
SOD1	AGGGCATCATCAATTTCGAG	ACATTGCCCAAGTCTCCAAC
SOD2	GGAAGCCATCAAACGTGACT	ACACATCAATCCCCAGCAGT
SRXN1	CATCGATGTCCTCTGGATCA	CTGCAAGTCTGGTGTGGATG
TRX1	CTGCTTTTCAGGAAGCCTTG	TGTTGGCATGCATTTGACTT
TXN2	TCAAGACCGAGTGGTCAACA	AATATCCACCTTGGCCATCA
TXNDC14	GGACAAGAGGGTCACTTGGA	AGGGTAGGGAGTTGCTTGGT
ACSL5	CTCAACCCGTCTTACCTCTTCT	GCAGCAACTTGTTAGGTCATTG
ACSL4	ACTGGCCGACCTAAGGGAG	GCCAAAGGCAAGTAGCCAATA
CPT1C	GGCAAGAGCTTCATCCGAC	TCATAAGTCAGGCAGAATTGACC
DECR1	GGAGGTACTGGCCTTGGTAA	AAACATCCATCTTCCGGCTG
ACADS	AGGGCGACTCATGGGTTCT	GGGATGCGACAGTCCTCAAAG
APOL3	GGTGGTCAAGCAGAGAGAAC	ATCCAGTGCAAGGAAGATGC
HADHA	ATATGCCGCAATTTTACAGGGT	ACCTGCAATAAAGCCTGG
ECI2	ATGGGACGCATGGAATGCC	TTCAAACCCAGTTGATTTCCTGT
ACADL	TCAGAGCATCGGTTTCAAAGG	AGGGCTCGGTTAGACAGAAAG
GAPDH	ACCCAGAAGACTGTGGATGG	TTCAGCTCAGGGATGACCTT

Table 2. List of antibodies

Antibody	Source	Catalog
Catalase	Cell signaling	#12980
GPX1	Cell signaling	#3206
GPX4	Abcam	ab125066
IDH2	Cell signaling	#56439
SOD2	Millipore	06-984
G6PD	Santa cruz	sc-373887
PGD	Cell signaling	#13389
PHGDH	Abcam	ab57030
SHMT2	Cell signaling	#12762
MTHFD2	Cell signaling	#41377
Prx2	Abcam	ab109367
Prx3	Abcam	ab73349
FoxM1	Cell signaling	#5436

III. RESULTS

1. CSCs exhibited metabolic reprogramming

We had previously reported a cell subpopulation, adapted to chronic metabolic stress, exhibiting cancer stem-like characteristics [46-48]. Accordingly, we used stem-like cancer cells (S-cells) derived from the human gastric cancer cell lines MKN1 and AGS as a model system for gastric CSCs.

I first compared the expression of central metabolism genes between P- and S-cells, using a PCR array. Compared to P-cells, S-cells exhibited general repression of metabolic pathway genes. However, genes of the fatty acid oxidation and one-carbon pool related purine nucleobase synthesis pathways were coordinately upregulated in S-cells (S-MKN1 and S-AGS, respectively) (Figure 1A). These data confirmed that S-cells display reprogrammed metabolic activities. I further validated the protein expression of corresponding mRNAs between P- and S-cells under various metabolic stress conditions. Of note, the specific genes and modules that were differentially expressed varied between the two subtypes of CSCs (S-MKN1 and S-AGS; Figure 1B). Among others, antioxidant enzymes such as SOD2, GPX4 and catalase were most prominently differently expressed between the two CSCs; while Prx3 expression was increased in both CSCs. Similarly, G6PDH in oxidative PPP, and PHGDH, SHMT2 and MTHFD2 in 1 carbon metabolism were increased only in S-AGS while IDH2 of mitochondrial NADPH producing enzyme was increased in

S-MKN1 alone, indicating heterogeneous metabolic properties in CSCs (Figure 1B).

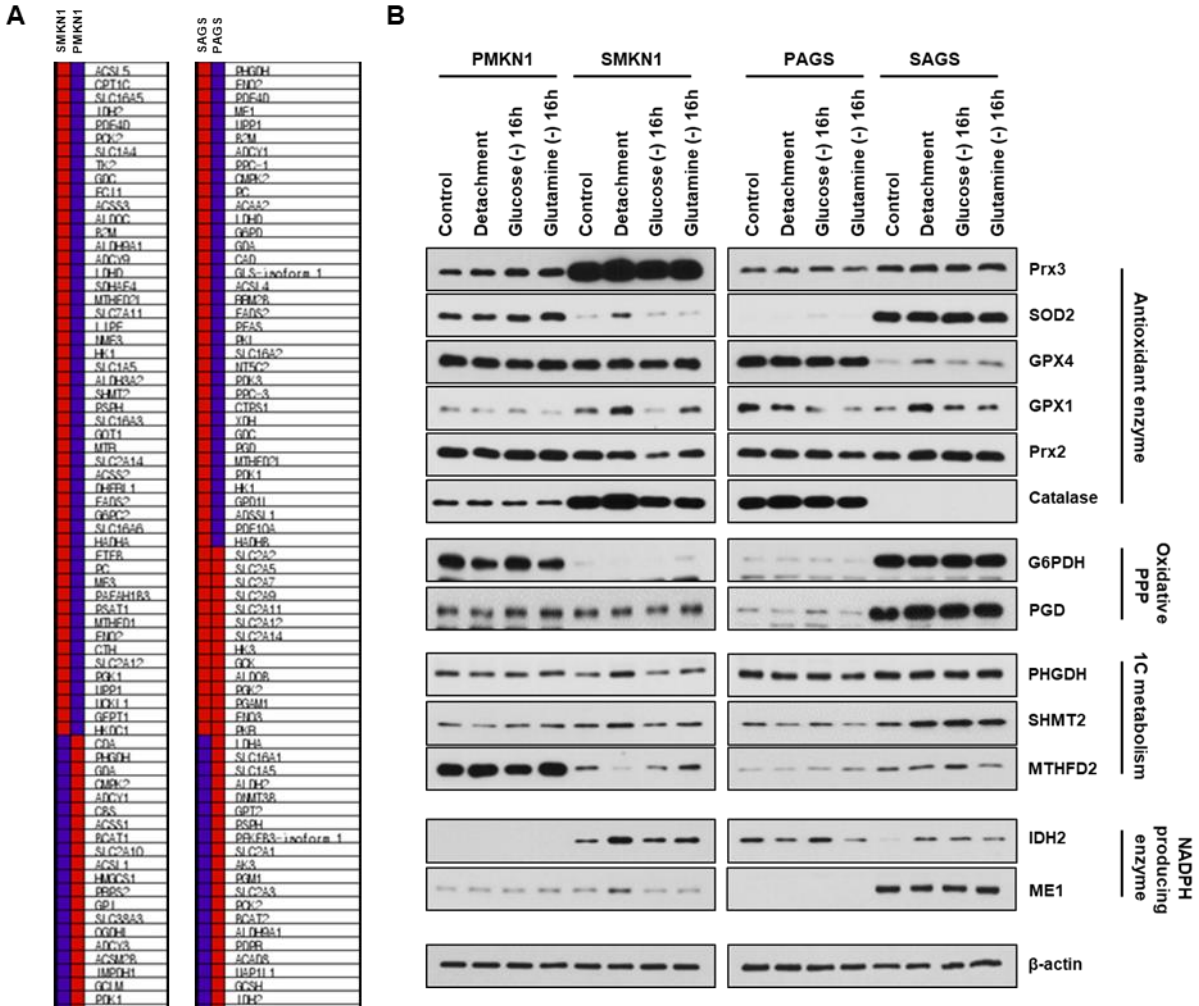

Figure 1. Stem-like cancer cells show transcriptomic reprograming associated with distinct metabolic phenotypes. (A) RNA was extracted, reverse transcribed, and analyzed by NuRNATM Human Central Metabolism PCR Array. Heatmap of transcript levels of central metabolism genes in parental cells and stem-like cancer cells. (B) Immunoblot analysis of key proteins among antioxidant enzymes, oxidative pentose phosphate pathway, 1C metabolism, and NAPDH-producing enzymes in CSCs compared with parental cells.

2. CSCs showed increased mitochondrial OXPHOS rather than glycolysis

Accumulating evidence suggests that mitochondrial biogenesis is crucial for CSC maintenance and chemotherapy resistance in several tumor types [3,50-53]. To assess mitochondria-prone metabolic reprogramming in CSCs, I examined the metabolic features related to mitochondrial function. Indeed, S-cells displayed reduced glucose uptake and lactate production in comparison to P-cells (Figure 2A-B). In contrast, S-cells exhibited an increased mitochondrial mass and DNA content (Figure 2C-D), indicating that mitochondrial biogenesis is activated. Consistently, S-cells demonstrated heightened mitochondrial membrane potential, evident from an increased amount of aggregated JC-1 dye and mitochondrial oxygen consumption (Figure 2E-F). Together, these results indicated that CSCs display distinct metabolic features that are more compatible with mitochondrial oxidative energy metabolism than found in P-cells.

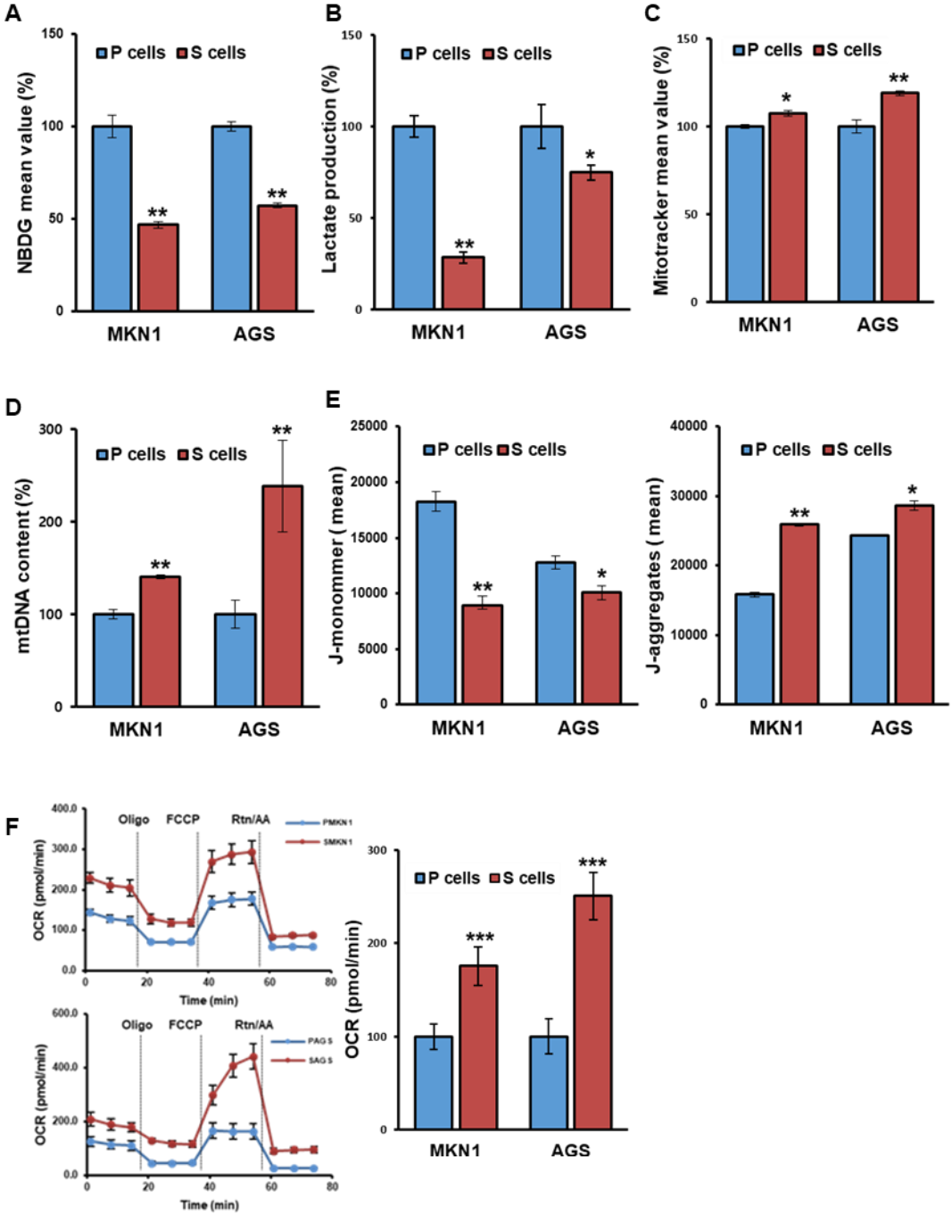

Figure. 2. Gastric CSCs display metabolic features compatible with oxidative metabolism. (A–F) Glucose uptake by 2-NBDG incorporation measured by flow cytometry (A), lactate production (B), mitochondrial mass as determined by flow cytometry using MitoTracker Green-FM (C), mitochondrial DNA (mtDNA) content (D), membrane potential (E), and oxygen consumption rate (F) in parental and selected stem-like cells from the MKN1 and AGS gastric cancer cell lines. Error Bars represent standard deviation. Statistical significance was determined by student`s T-test. All experiments were performed in triplicates or quadruplicates. *** indicates P-value < 0.001.

3. CSCs have reduced ROS levels

Increased OXPHOS and ROS levels are inherently linked. To investigate ROS levels in CSCs, I measured the mitochondrial superoxide levels using MitoSOX Red. Lower levels of superoxide (based on MitoSOX Red) staining were found in S-cells of both cell lines compared to those of their corresponding P-cells (Figure 3A-B). Similarly, dichloro-dihydro-fluorescein diacetate (DCFH-DA) fluorescence detection (as a marker of intracellular hydrogen peroxide) revealed decreased ROS levels in S-cells (Figure 3C). Furthermore, immunofluorescence analysis revealed that S-cells generally had reduced ROS levels both in the mitochondria and cytosol compared to P-cells (Figure 3D–E).

To exclude the possibility of an idiosyncratic reduction of ROS in S-cells, I confirmed the ROS levels in CSC subpopulation from P-cells, sorted by CD44 and CD133. $CD44^{+}CD133^{+}$ high-expressing cells (CSCs) displayed decreased mitochondrial ROS levels in comparison to $CD44^{-}CD133^{-}$ cells (non-CSCs; Figure 3F–G). To further confirm these findings in gastric CSCs are general characteristics, breast CSCs were subject to ROS measures [54,55]. Indeed, S-MCF7 displayed lower ROS levels than the parental cells (P-MCF7) (Figure 3H). Likewise, breast CSCs were sorted by flow cytometry to determine ROS levels. The two BCSC subtypes, $CD24^{-}CD44^{+}$ M-BCSCs and $ALDH^{+}$ E-BCSCs, showed a low ROS phenotype compared to the non-CSC population (Figure 3I-J).

Together, these results indicated that maintenance of low ROS levels might be a universal metabolic feature of CSCs.

A CSC phenotype is a well-known feature among numerous chemotherapy-resistant tumors [56] and most chemotherapeutics generate ROS in cancer cells [57]. Concurrent with this general phenomenon, S-cells displayed reduced sensitivity than P-cells to the anticancer drug 5-fluorouracil (5-FU), which is widely used in gastric cancer treatment (Figure 3K). Moreover, ROS levels increased after 5-FU treatment in P-cells, in a dose-dependent manner, whereas relatively low levels of ROS were maintained in CSCs (Figure 3L-M). These findings suggested a link between ROS levels and 5-FU sensitivity in CSCs, indicating that CSCs may have a cell intrinsic drug resistant mechanism related to redox homeostasis.

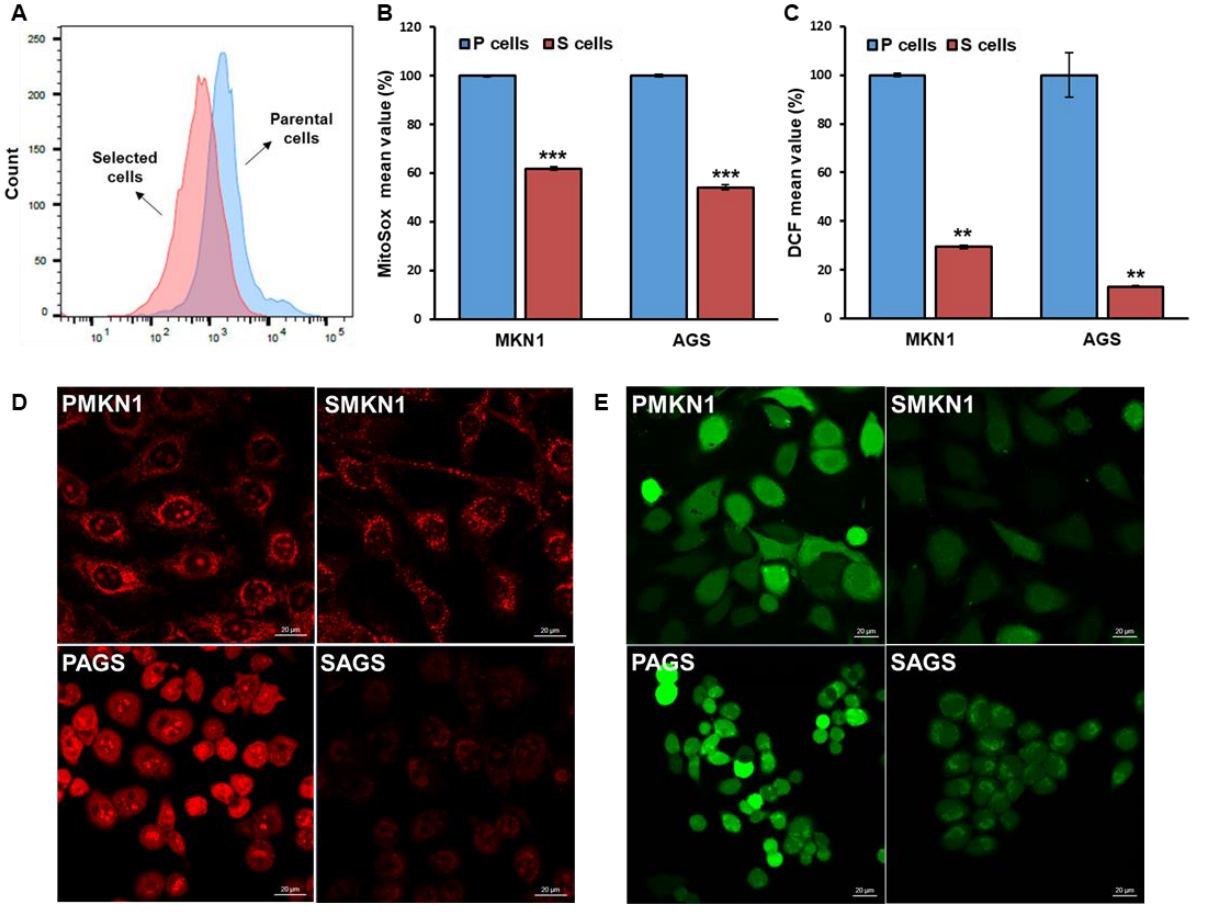

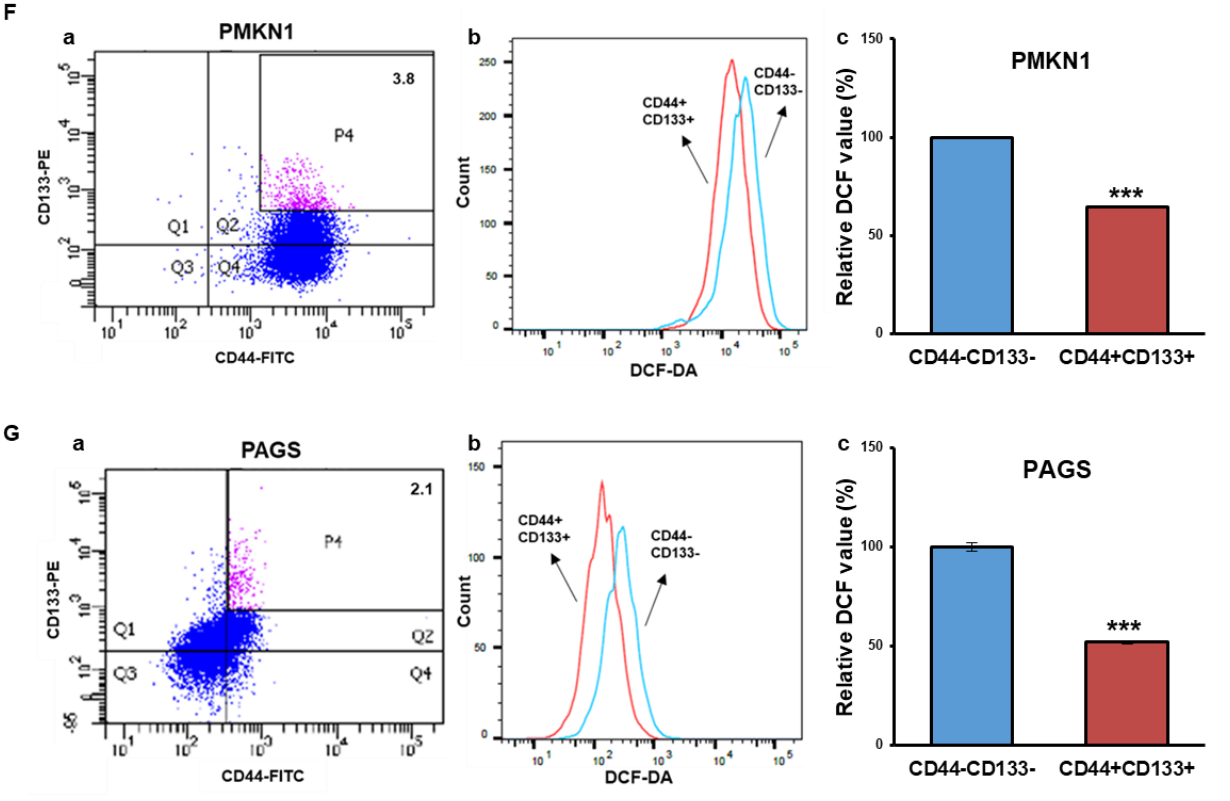

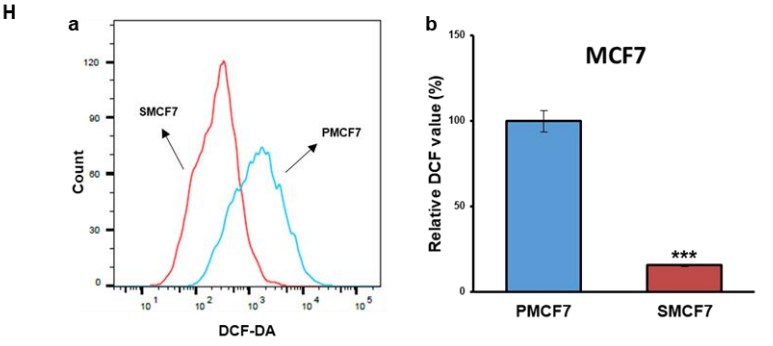

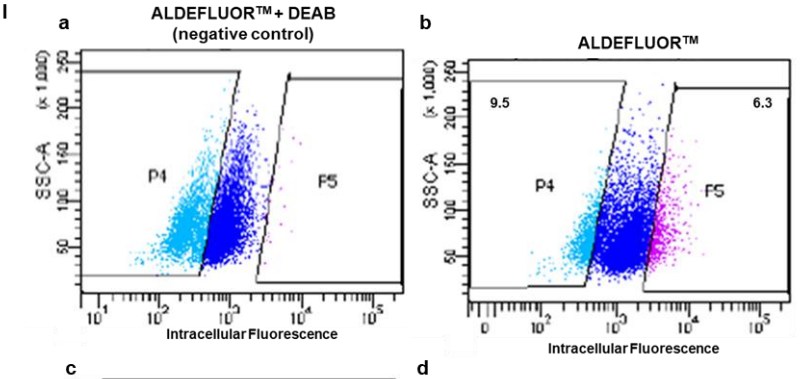

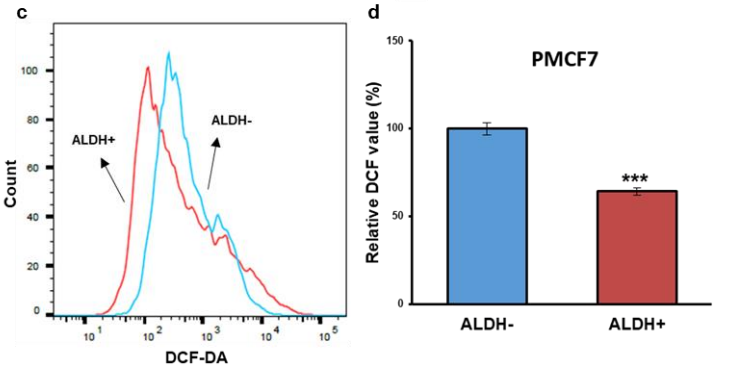

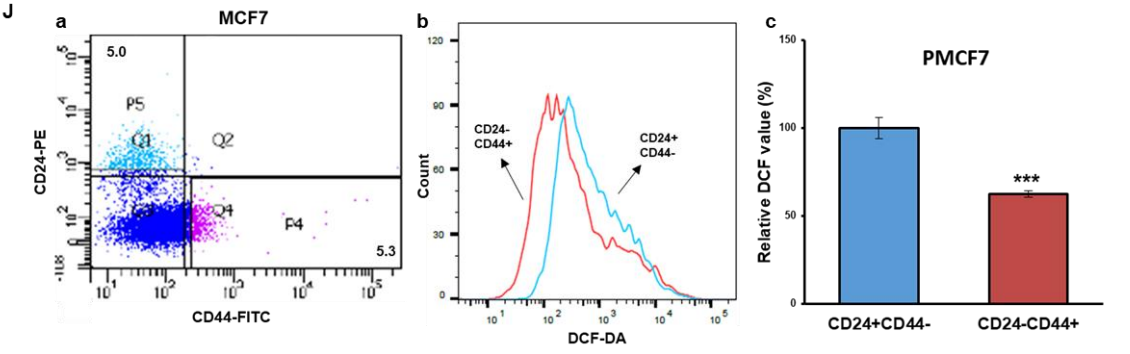

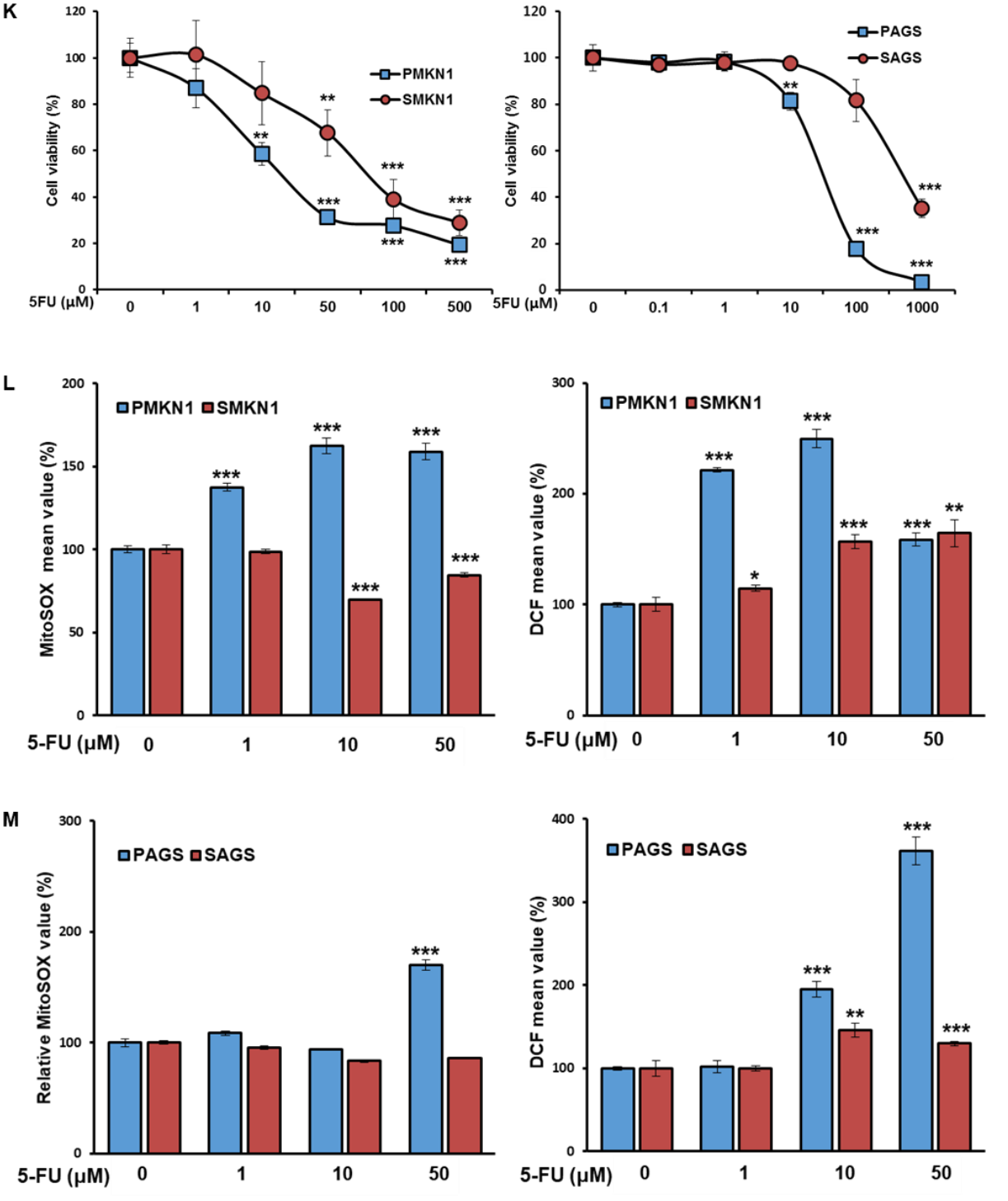

Figure 3. CSCs maintain low ROS levels compared with non-CSCs. (A) Levels of mitochondrial superoxide (B) and intracellular hydrogen peroxide (C) were measured by fluorescence-activated cell sorting after staining with Mito-Sox RED and DCFH-DA dye. (D–E) Representative confocal micrographs of immunofluorescence staining in parental cells and CSCs using Mito-Sox RED and DCFH-DA dye. (F–G) a. FACS profile of parental gastric cancer cells from which $CD44^{+}CD133^{+}$ cells (CSC-enriched population) and $CD44^{-}CD133^{-}$ cells (non-CSCs) were isolated by flow cytometry. b. DCF-DA histograms for the two populations from (a). c. Mean and SEM for replicates of (b). (H) DCFH-DA fluorescence in Parental and Selected MCF7. (I) $ALDH^{+}$ and $ALDH^{-}$ populations were sorted in MCF7 cells using FACS and ROS levels were measured in both populations. (J) $CD24^{-}CD44^{+}$ and $CD24^{+}CD44^{-}$ populations were sorted in MCF7 cells using FACS and ROS levels were measured in both populations. (K) Parental cells and cancer stem-like cells were treated with 5-FU for 72 hours; cell viability was determined with MTS. (L–M) CSCs and non-CSCs were treated with the indicated doses of 5-FU for 72 h. Levels of mitochondrial ROS were measured by Mito-Sox RED staining (L). Levels of intracellular ROS measured by DCFH-DA fluorescence (M). Statistical significance was determined by student`s T-test. All experiments were performed in triplicates or quadruplicates. *** indicates P-value < 0.001.

4. FoxM1 transcriptionally activated Prx3 in gastric CSCs

Cancer cells have developed antioxidant mechanisms to protect themselves from oxidative stress by expressing various detoxifying enzymes such as superoxide dismutase, catalase, glutathione peroxidases, and peroxiredoxins [58].

To determine whether ROS detoxification genes increase in stem-like cancer cells and contribute to selective advantages, I detected the mRNA expression of key ROS detoxification genes through reverse transcription-quantitative PCR. Catalase and peroxiredoxin 3 (Prx3) mRNAs were highly upregulated in S-MKN1 cells (Figure 4A). Consistently, mitochondrial Prx3 protein was upregulated in S-cells compared to that in P-cells (Figure 4B).

Prx3 is reported to be transcriptionally upregulated by the transcription factor FoxM1 [43,58]. To investigate the regulation of Prx3 expression in S-cells, I analyzed the expression and nuclear localization of FoxM1. Indeed, the expression levels and nuclear localization of FoxM1 were increased in S-cells compared to those in P-cells (Figure 4C–E). In contrast, FoxM1 siRNA-transfected cells displayed Prx3 downregulation in comparison to control siRNA cells (Figure 4F–G). Additionally, stable knockdown of FoxM1 by shRNA also shoId Prx3 downregulation (Figure 4H) and overexpression of FoxM1 increased Prx3 expression (Figure 4I). Furthermore, FoxM1 and Prx3 were upregulated in $CD44^{+}CD133^{+}$ isolated gastric cancer cells that in

$CD44^{-}CD133^{-}$ cells (Figure 4J). I also utilized thiostrepton, a selective FoxM1 inhibitor, that reduced FoxM1 and Prx3 expression (Figure K). Together, these results confirmed the mechanistic association between FoxM1 and Prx3 expression in gastric CSCs.

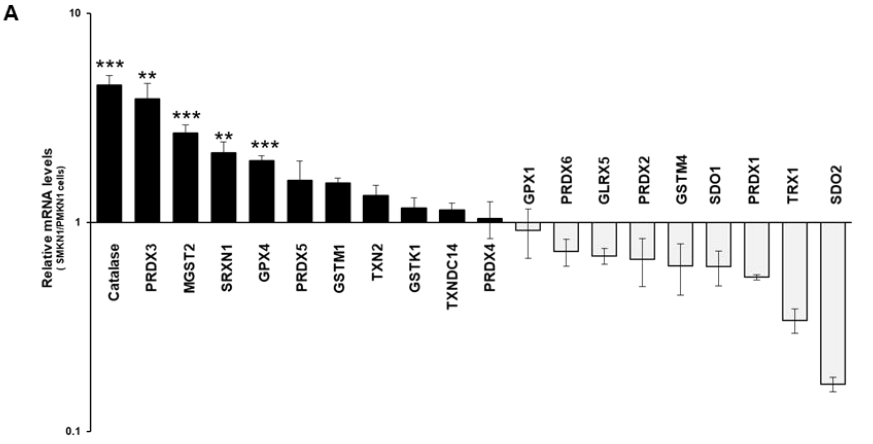

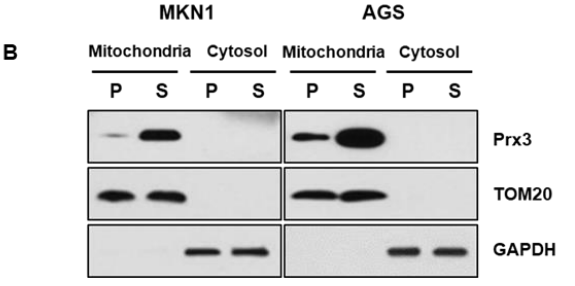

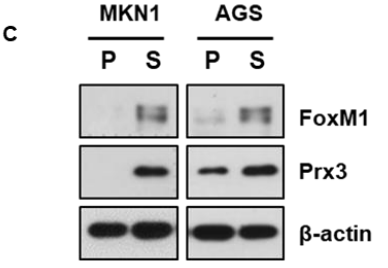

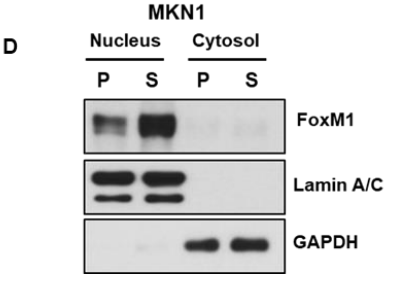

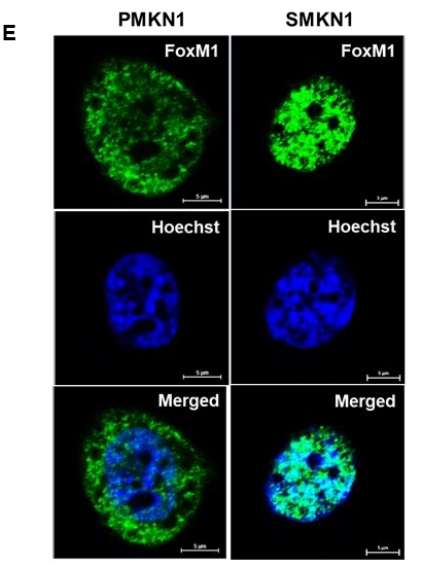

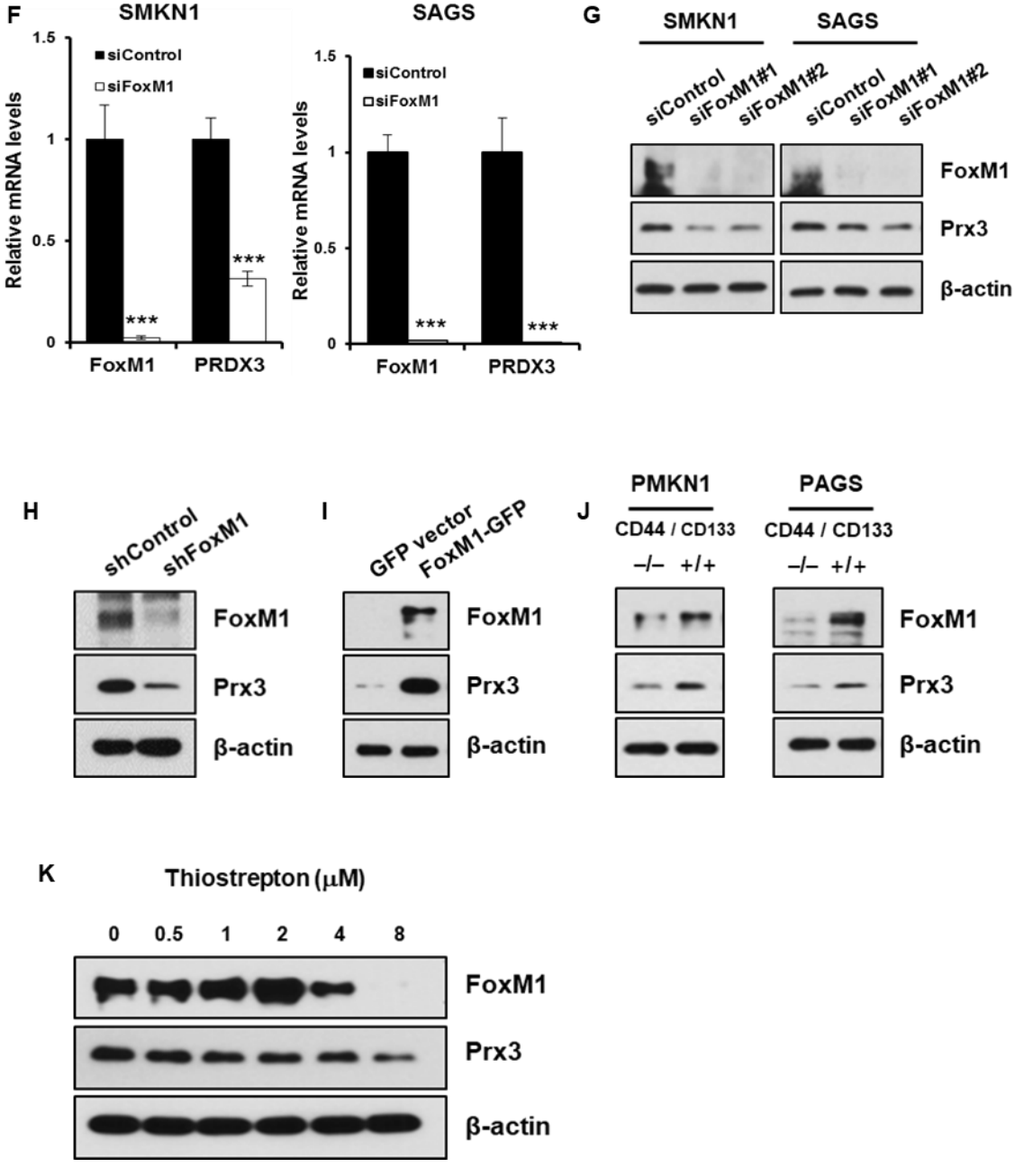

Figure 4. FoxM1 increases Prx3 expression and in CSCs. (A) mRNA expression levels of ROS detoxification genes in parental cells (P-MKN1) and stem-like cancer cells (S-MKN1). (B) Mitochondrial and cytoplasmic levels of Prx3 in parental cells and CSCs. (C) Immunoblot analysis of FoxM1 and Prx3 levels in parental cells and CSCs. (D–E) Cytoplasmic and nuclear levels of FoxM1 in parental cells and CSCs. (F) Prx3 mRNA expression, as determined by quantitative fluorescence PCR, in cells transfected with siRNA against FoxM1 and control siRNA. (G-H) FoxM1-depleted cells showed downregulation of Prx3 expression. (I) FoxM1-overexpression cells showed upregulation of Prx3 expression based on western blot analysis with the indicated antibodies. (J) FoxM1 and Prx3 expression confirmed by western blotting of $CD44^{-}CD133^{-}$ and $CD44^{+}CD133^{+}$ non-CSC subpopulations. (K) SMKN1 cells were treated with thiostrepton, a potent FoxM1 inhibitor, and expression of CD133 and Prx3 protein levels were determined by western blot. Statistical significance was determined by student`s T-test. All experiments were performed in triplicates or quadruplicates. *** indicates P-value < 0.001.

5. The transcription factor FoxM1 is required for redox homeostasis and survival of gastric CSCs against chemotherapeutics

FoxM1 is suggested to regulate intracellular ROS levels, thus protecting cancer cells from oxidative stress [58,59]. Based on this link between FoxM1 and the mitochondria-specific antioxidant enzyme Prx3 in S-cells, I next explored the role of FoxM1 in regulating ROS homeostasis in relation to cell fitness. As expected, intracellular ROS concentrations were significantly increased in FoxM1-depleted cells, whereas treatment of FoxM1-depleted cells with the antioxidant *N*-acetylcysteine (NAC) substantially restored the ROS levels (Figure 5A). Similarly, mitochondrial ROS levels were significantly higher in FoxM1-depleted cells, and MitoTEMPO, a specific scavenger of mitochondrial superoxide, efficiently suppressed the ROS accumulation in FoxM1-depleted S cells (Figure 5B).

FoxM1 reportedly plays important roles in drug resistance [60,61]. To investigate the potential association between drug resistance and the capability of FoxM1 to mitigate oxidative stress induced by anticancer drugs, I analyzed the effect of chemotherapy in CSCs. Cell death was detected via immunoblotting for cleaved caspase-3, a marker of apoptosis, after treatment with different concentrations of 5-FU in FoxM1 siRNA-transfected S-cells (Figure 5C). Moreover, treatment with NAC substantially rescued 5-FU-induced cell death (Figure 5D).

Together, these data showed that elevated ROS levels are associated with increased cell death after exposure to chemotherapeutics in CSCs, implying FoxM1-mediated ROS down-modulation as a mechanism underlying drug resistance.

Clinically, FoxM1 was upregulated in patients with malignant gastric cancer compared to that in the adjacent normal or benign inflamed tissues (Figure 5E). Further, FoxM1 upregulation predicted poor survival in patients with various types of cancers, including gastric, breast, lung, and ovarian cancers (Figure 5F).

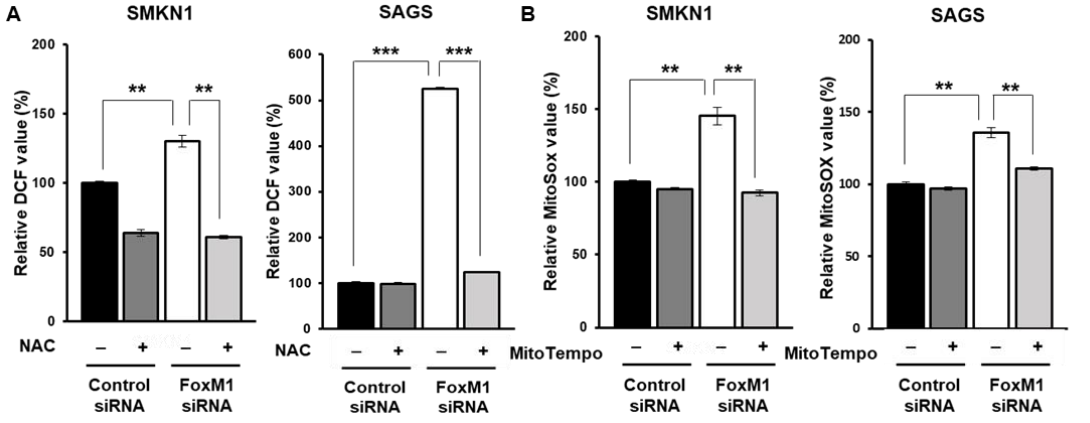

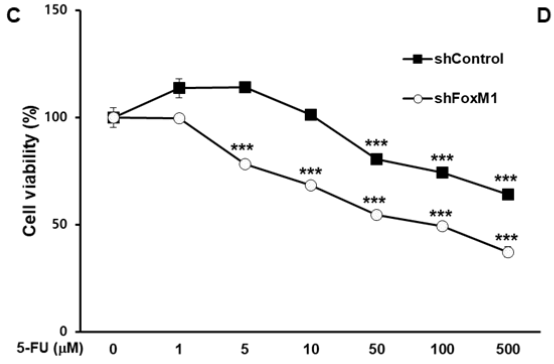

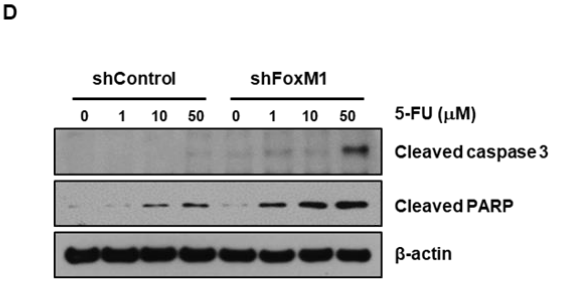

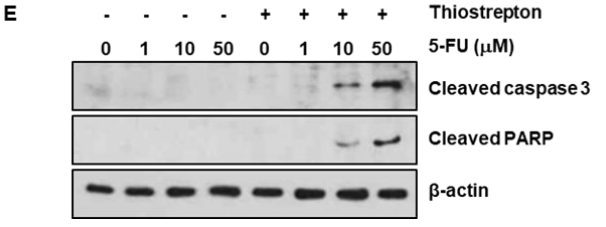

F

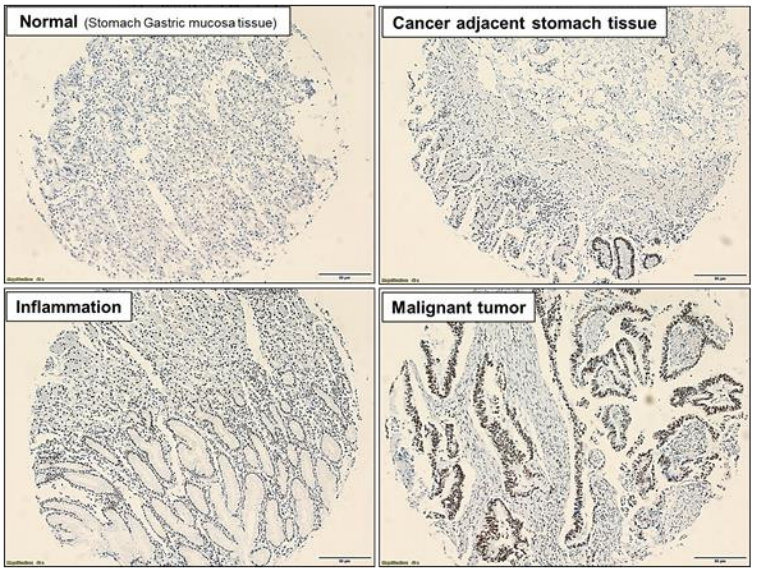

H

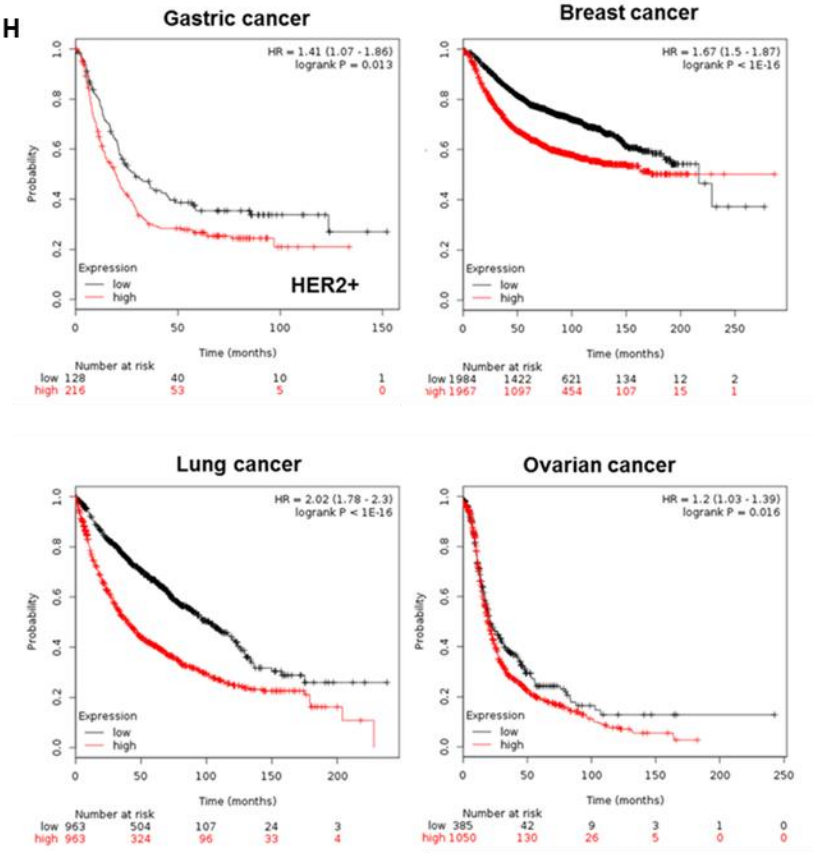

Figure 5. FoxM1 mediates drug resistance through reducing mitochondrial ROS in CSCs. (A–B) CSCs were transfected with control or FoxM1 siRNA for 72 h. Intracellular ROS levels were measured using DCF-DA at baseline and upon supplementation with NAC (A), and mitochondrial ROS levels were measured using MitoSOX at baseline and upon supplementation with MitoTempo (B). (C) Cell viability of FoxM1 knockdown and control cells treated with indicated concentrations of 5-FU (n=3). (D) Western blot assay of cleaved caspase-3 and cleaved PARP in control and FoxM1 knockdown cells treated with indicated concentrations of 5-FU. (E) Western blot assay of cleaved caspase-3 and cleaved PARP in SMKN1 cells upon 50FU and thiostrepton treatment at indicated concentrations. (F) Expression of FoxM1 in gastric cancer tissues and adjacent normal tissues from patients determined by immunohistochemistry. (G) FoxM1 levels correlated with poor patient survival in gastric cancer, breast cancer, lung cancer and ovarian cancer. Statistical significance was determined by student`s T-test. All experiments were performed in triplicates or quadruplicates. *** indicates P-value < 0.001.

6. CSCs have increased mitochondrial NADPH production

The function of ROS-quenching enzymes, including Prx3, requires cellular reducing power. NADPH, the primary source of cellular reducing power, serves as an electron carrier to maintain redox homeostasis and reductive biosynthesis, with compartmentalized cytosolic and mitochondrial pools to facilitate reduction reactions at corresponding sites [62].

Indeed, intracellular NADPH levels were higher in CSCs, and was associated with an increase in reduced glutathione levels (Figure 6A–6B). PCR array analysis (Figure 1A) revealed that genes encoding some NADPH-generating enzymes (e.g., *IDH2, ME3, MTFHD2L, MTHFD1, ME1,* and *G6PD*) were upregulated in both CSC subtypes in comparison to their respective P-cells. Single-sample gene enrichment analysis (ssGSEA) of PCR array result identified the mitochondrial fatty acid beta-oxidation pathways were significantly enriched in S-MKN1 cells while one carbon pool by folate and related purine nucleotide biosynthesis pathways as well as PPP were enriched in S-AGS cells (Figure 6C). Indeed, inspection on differential gene expressions by volcano plots showed essential genes in FAO (e.g., *ACSL5, ECI1,* and *CPT1C*) were coordinately upregulated in S-MKN1 cells. Most differentially expressed genes in S-AGS over P-AGS were *PHGDH, ME1* and *G6PDH* confirming the ssGSEA results (Figure 6D). To assesses the protein expression of corresponding

genes, we performed immunoblotting and showed IDH2 and MTHFD2 were increased in S-MKN1 and S-AGS, respectively (Figure 6E).

Therefore, both S-MKN1 and S-AGS cells displayed increased levels of mitochondrial enzymes compared to their parental counterparts, playing major roles in regenerating NAPDH from $NADP^+$, mitochondrial isocitrate dehydrogenase (IDH2), and mitochondrial methylene tetrahydrofolate dehydrogenase (MTHFD2), respectively.

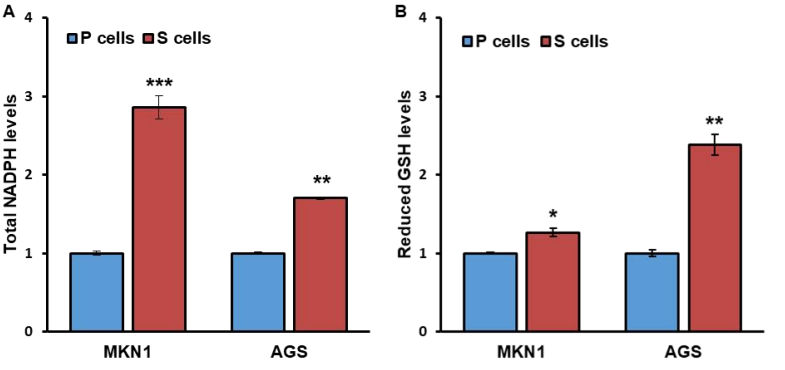

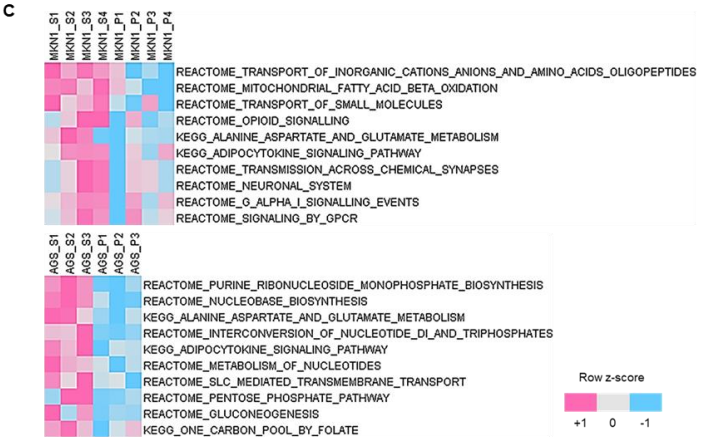

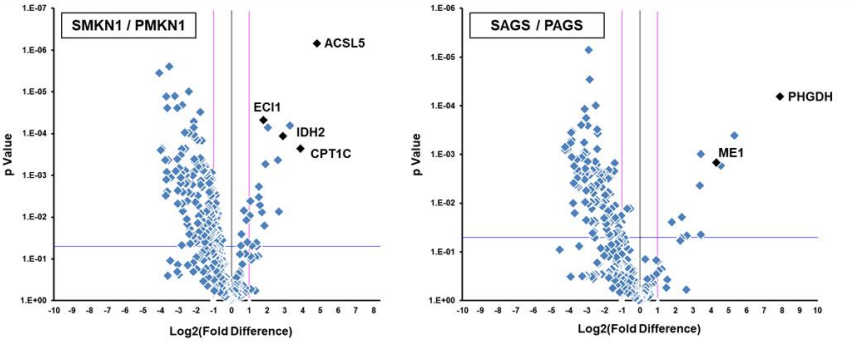

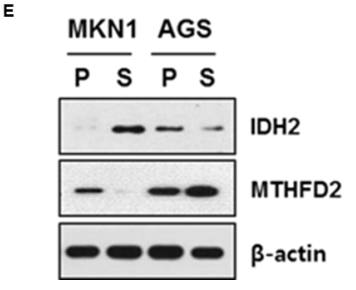

Figure 6. Mitochondrial NADPH regeneration increases in CSCs. (A) Total intracellular NADPH levels in non-CSCs and CSCs (n = 3). (B) Reduced glutathione levels in non-CSCs and CSCs (n = 3). (C) Single-sample gene set enrichment analysis (ssGSEA) with rank normalization method was performed on the PCR array result. It determines whether a predifend gene set is enriched at the top or bottom of the pre-ranked gene list for each sample. Molecular Signatures Database (MSigDB) gene sets curated from the KEGG and Reactome pathway database were used. The canonical pathways of which average enrichment score is greater at the S cells are sorted by p-value from student's t-test. (D) A total of 373 transcripts involved in cell metabolism are depicted in a volcano plot. The pink lines indicate a fold-change threshold of 2, and the blue lines indicate the P-value cut-off (P = 0.05). (E) Immunoblot analysis of IDH2 and MTHFD2 levels in parental cells and CSCs. Statistical significance was determined by student`s T-test. All experiments were performed in triplicates or quadruplicates. *** indicates P-value < 0.001.

7. CSCs have enhanced fatty acid oxidation

In cancer cells, fatty acid oxidation (FAO) is an important source of mitochondrial NADPH by generating acetyl-CoA to sustain the TCA cycle [63]. To analyze how CSCs utilize nutrients, I performed uniformly-labeled [U-^{13}C]glucose and [U-^{13}C]palmitate flux analyses using liquid chromatography-mass spectrometry (LC-MS) using cell extracts. Interestingly, the glucose-derived ^{13}C signal was significantly reduced among TCA cycle intermediates, including citrate, α-ketoglutarate (α-KG), and malate in S-MKN1 cells, compared to those in P-MKN1 cells (Figure 7A). Furthermore, S-AGS cells had reduced citrate, malate, and succinate levels, although α-KG was not detected (Figure 7B). However, mass distribution analysis revealed an increase in m+2 citrate and malate in S-MKN1 cells, suggesting that FA-derived carbons sustained the oxidative TCA cycle in CSCs (Figure 7C–D).

Furthermore, the mRNA expression levels of key genes associated with FAO were upregulated in CSCs (Figure 7E), whereas the protein levels of ACC1, which produces malonyl-CoA to directly inhibit CPT1, were decreased in CSCs (Figure 7F).

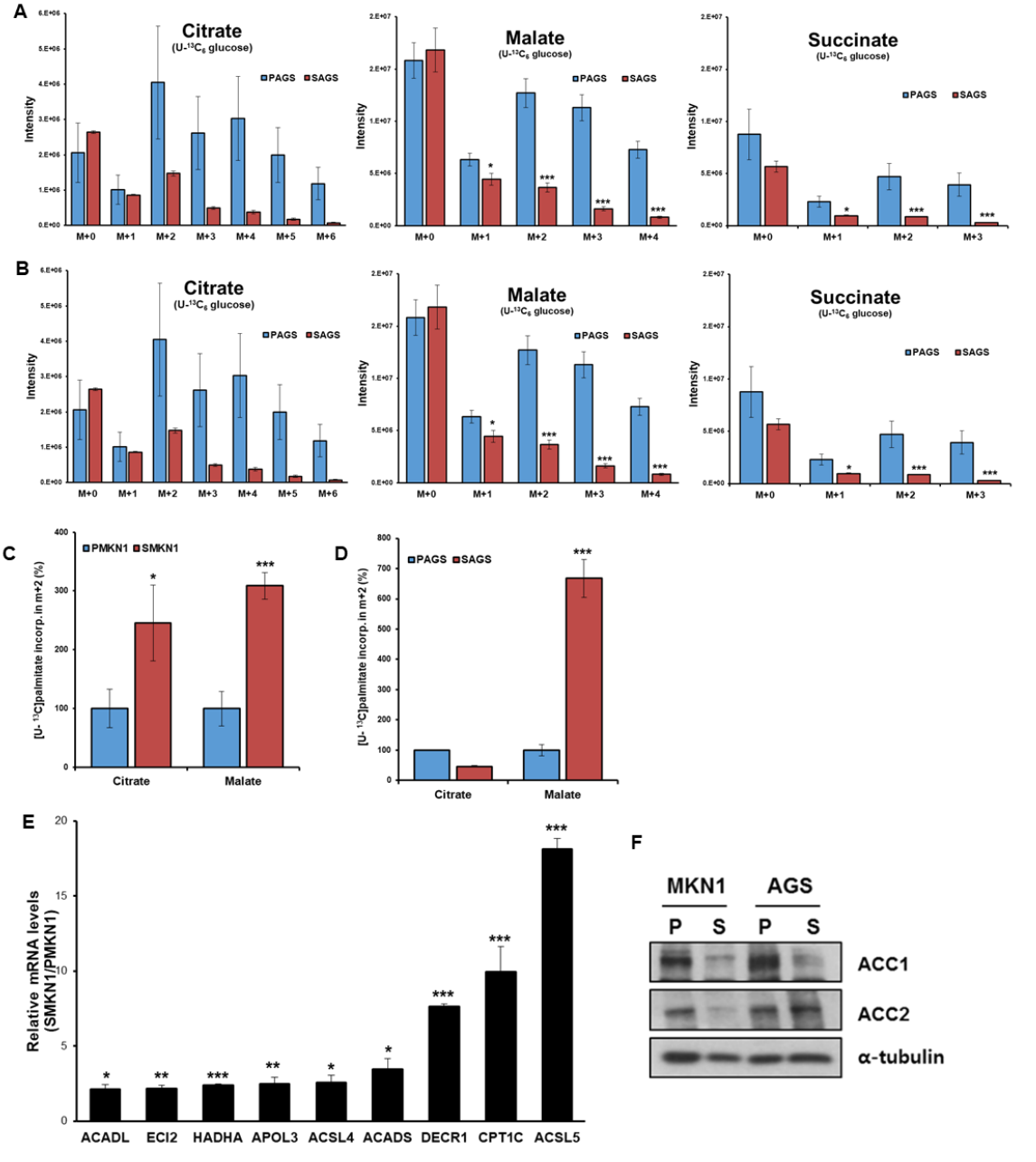

Figure 7. Enhanced fatty acid oxidation in CSCs. (A-D) CSCs and non-CSCs cultured in RPMI media containing no glucose plus 10% dialyzed fetal bovine serum was respectively traced with 5.5mM U-13C glucose and 100 μM U-13C palmitate for 16 h. Relative isotopolog distribution of the indicated metabolites measured by LC-MS. n = 3. FC, fold-change in glucose /palmitate-derived (13C ≥ 2) metabolite abundance relative to in parental cells. (E) Real-time PCR analysis assessing the expression of key lipid metabolism genes in S-MKN1 cells. (F) Immunoblot analysis of ACC1 and ACC2 protein expression in CSCs versus non-CSCs. Statistical significance was determined by student`s T-test. All experiments were performed in triplicates or quadruplicates. *** indicates P-value < 0.001.

8. FAO-mediated NADPH regeneration is a reversible cause of drug resistance in CSCs

Since NADPH, which is required to quench ROS, is generated through FAO, I hypothesized that FAO is associated with the mechanism underlying drug resistance in CSCs. To determine the contribution of FAO to 5-FU-acquired resistance, CSCs were treated with 5-FU in combination with the FAO inhibitor etomoxir. Etomoxir and 5-FU exhibited synergistic effects to significantly decrease CSC viability (Figure 8A).

FAO is reportedly important for cells that have become detached from the extracellular matrix and those cultured in nutrient-deprived conditions[64,65]. To confirm the role of FAO-NADPH-ROS pathway herein, I examined the effects of matrix detachment on ROS production. Extracellular matrix detachment significantly increased ROS levels in both CSCs and non-CSCs; however, the magnitudes of these increases were relatively lower in CSCs (Figure 8B). Similarly, ROS levels were lower in CSCs under glucose-deprived conditions (Figure 8C) and higher in those treated with etomoxir (Figure 8D). These results also implied that FAO-mediated ROS homeostasis is associated with key features including CSC invasion and metastasis.

To investigate the role of mitochondrial NADPH-producing enzymes in CSCs, I depleted mitochondrial NAPDH-producing enzymes with siRNAs, which significantly decreased NADPH levels and was associated with increased

mitochondrial ROS levels in CSCs (Figure 4J–M). Furthermore, FAO inhibition with etomoxir, an irreversible CPT1 inhibitor, more significantly reduced NADPH levels and increased mitochondrial ROS levels in CSCs. Thus, FAO, via IDH2 or MTHFD2, substantially contributes to physiologically significant mitochondrial NADPH production.

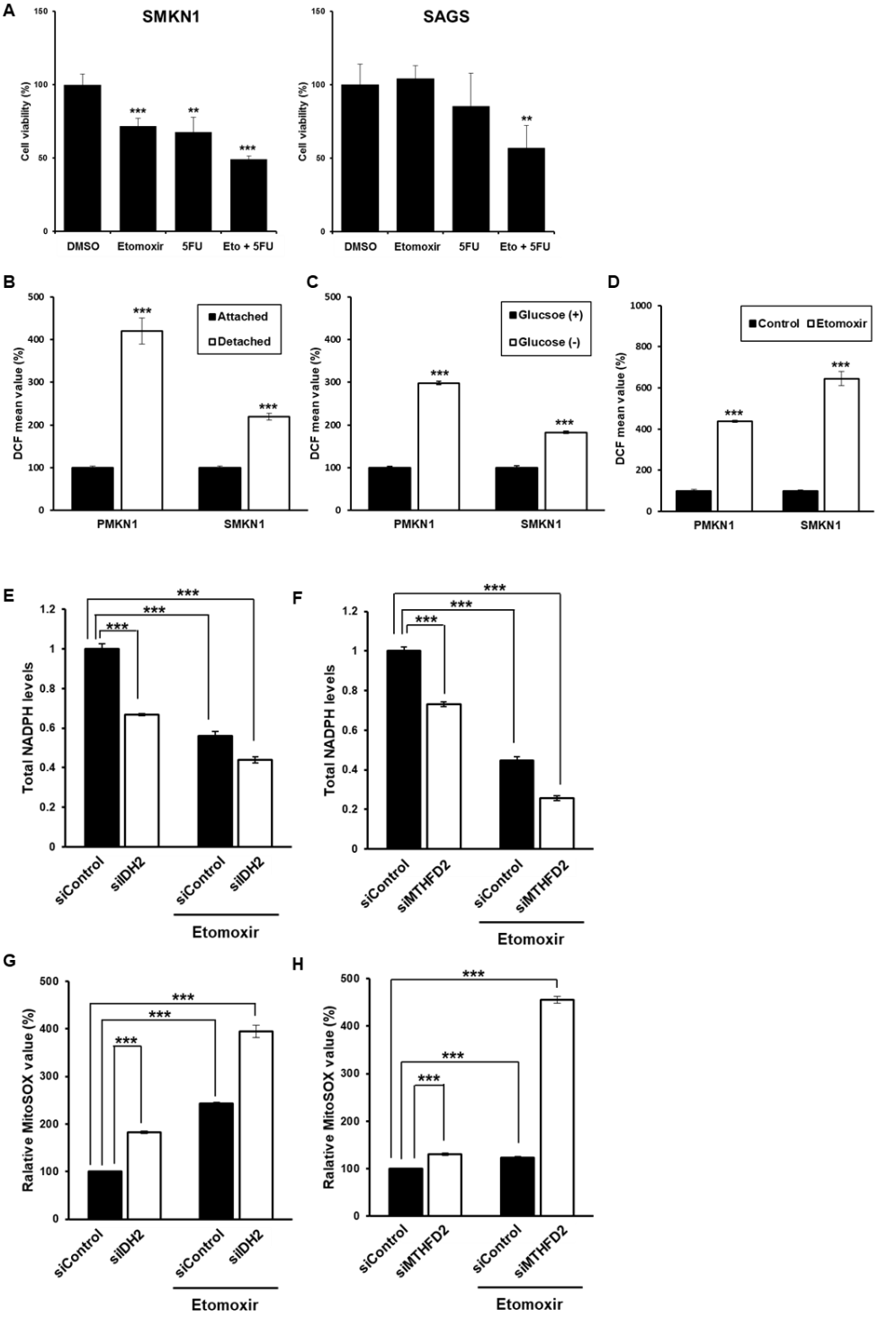

Figure 8. FAO-mediated NADPH regeneration in CSCs. (A) Cell viability assay showing etomoxir sensitizes CSCs to 5-FU. (B) Effects of matrix detachment on CSCs and non-CSCs. ROS were measured in the indicated cells at 24 h after plating in adherent or non-adherent (poly-HEMA-coated) plates using DCFH-DA. Cellular ROS levels after glucose deprivation (C) and treatment with etomoxir (D) were determined by DCFH-DA flow cytometry analysis.

(E–H) Total intracellular NADPH levels (J–K, n = 3) in control and deletion of IDH2 or MTHFD2 in CSCs and mitochondrial ROS levels (L-M, n = 3) in control and deletion of IDH2 or MTHFD2 in CSCs, in baseline and upon supplementation with etomoxir. Statistical significance was determined by student`s T-test. All experiments were performed in triplicates or quadruplicates. *** indicates P-value < 0.001.

IV. DISCUSSION

Tumor cells reprogram their metabolic pathways to adapt to the fluctuating metabolic environment. CSCs have evolved a flexible energy metabolic strategy to increase fitness in the ever-changing tumor microenvironment. In particular, to cope with the uncertainty in securing nutrients and appropriate energy substrates, CSCs harness OXPHOS as the dominant metabolic strategy, which is far more efficient than glycolysis but comes at a cost of overproduced ROS, thereby requiring large amounts of NADPH as a counteractive measure [66].

Although physiologically important, beyond a certain level, ROS can damage the cellular functions of cancers by subjecting them to oxidative stress. Thus, the maintenance of ROS at appropriate levels is imperative for regulating the stemness-associated properties of cancer cells [67]. This was confirmed in our CSC model, wherein both CSC lines displayed activated mitochondrial OXPHOS and maintained relatively low ROS levels to sustain their functions.

Scavenging of ROS is mediated by a set of antioxidant enzymes expressed in various subcellular compartments [68]. During adaptation to metabolic stress, our selected CSCs (S-cells) displayed metabolic remodeling of numerous antioxidant enzymes including catalase, superoxide dismutase 2, Gpxs, and Prxs. In particular, Prx3 levels were substantially increased as a common factor in the two CSC subtypes. Recent studies have reported that mitochondrial Prx3, transcriptionally activated by FoxM1, maintains mitochondrial function by eliminating ROS produced upon ATP production in the OXPHOS system in

colonic CSCs[43]. Similarly, our stem-like cancer cells also primarily eliminated ROS via the FoxM1-Prx3 axis through ROS-quenching mechanisms

In general and in glycolytic tumors, including proliferating tumor cells, most of the cellular reducing power in the form of NADPH is generated through the pentose phosphate pathway or hexose monophosphate shunt. However, tumor cells, including the S-cells established herein, do not rely on glycolysis but rather maintain sufficiently high levels of NADPH to effectively neutralize ROS. To explore the potential sources of this NAPDH, I performed metabolomic flux analysis and found that S-cells utilize fatty acid-derived metabolites to generate NADPH. Furthermore, in absence of glucose, the S-cells were still viable and maintained ROS in the homeostatic range, suggesting that these S-cells use a different energy/nutrient substrate other than glucose. S-cells used fatty acid to feed the TCA cycle and generate NADPH, as is evident from metabolic flux analysis using stable isotope labeling for MS analysis.

Several recent studies have reported that mitochondrial IDH2 is essential for supplying the NADPH needed to defend cancer cells against mitochondrial oxidative damage and promote cell survival [69-71].

MTHFD2, which is frequently overexpressed in cancers [72] , also contributes to NADPH homeostasis [73]. Moreover, MTHFD2-mediated mitochondrial 1-carbon metabolism appears to be critical for cancer stem-like properties and drug resistance [74]. Notably, S-cells also appear to use different enzyme modules to generate NADPH. Differences have been observed between the two model cell

lines, with one line displaying IDH2-dependent NADPH regeneration and the other depending on MTHFD2.

A range of anticancer therapeutics, such as chemotherapy or ionizing radiation, involves increasing cellular ROS levels, which are effective against cancer cells [57]. Thus, tumor cells with intrinsic mechanisms to mitigate ROS production induced by chemotherapy or ionizing radiation can survive and become resistant to the anticancer therapy. Indeed, S-cells exhibited higher cell viability than P-cells upon 5-FU treatment, which was associated with lower ROS levels, indicating the crucial role of ROS in chemotherapy-induced cytotoxicity. When I knocked down FoxM1 in S-cells or supplemented the cells with NAC, a potent ROS detoxifying agent, reversion of cell viability was observed, further confirming the mechanistic link between ROS and the tumoricidal effect of 5-FU. Therefore, anticancer strategies are required to harness the mechanisms underlying intracellular ROS regulation, which can help overcome drug resistance and consequently enhance the clinical benefits of anticancer therapeutics.

Despite differences in specific enzyme modules that the two S-cell lines use for NADPH regeneration, they both belong to the TCA cycle or are mitochondria-dependent, suggesting that CSCs have a mitochondria-centric energy metabo-phenotype. However, further studies would be required to investigate the regulatory mechanisms of these enzymes in CSCs.

V. CONCLUSION

This study showed that CSCs exhibit increased OXPHOS, and paradoxically maintain a low level of ROS, through coupling of FoxM1-dependent Prx3 expression and FAO-mediated NADPH regeneration (Figure 9). Thus, a mitochondrial ROS homeostasis-targeted approach may be an effective strategy for controlling cancers that are refractory to conventional chemotherapy.

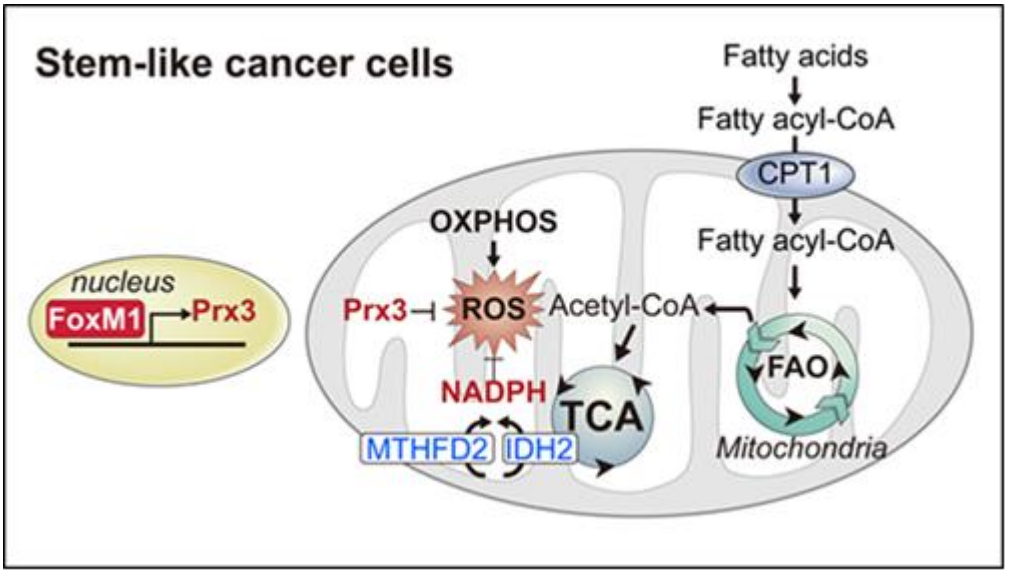

Figure 9. Schematic representation of ROS regulatory mechanism in CSCs

REFERENCES

1. Warburg O. On the origin of cancer cells. Science 1956;123:309-14.
2. Vander Heiden MG, Cantley LC, Thompson CB. Understanding the Warburg effect: the metabolic requirements of cell proliferation. Science 2009;324:1029-33.
3. Sancho P, Burgos-Ramos E, Tavera A, Bou Kheir T, Jagust P, Schoenhals M, et al. MYC/PGC-1alpha Balance Determines the Metabolic Phenotype and Plasticity of Pancreatic Cancer Stem Cells. Cell Metab 2015;22:590-605.
4. Dong C, Yuan T, Wu Y, Wang Y, Fan TW, Miriyala S, et al. Loss of FBP1 by Snail-mediated repression provides metabolic advantages in basal-like breast cancer. Cancer Cell 2013;23:316-31.
5. Lin CH, Hung PH, Chen YJ. CD44 is associated with the aggressive phenotype of nasopharyngeal carcinoma through redox regulation. Int J Mol Sci 2013;14:13266-81.
6. Janiszewska M, Suva ML, Riggi N, Houtkooper RH, Auwerx J, Clement-Schatlo V, et al. Imp2 controls oxidative phosphorylation and is crucial for preserving glioblastoma cancer stem cells. Genes Dev 2012;26:1926-44.
7. Vlashi E, Lagadec C, Vergnes L, Matsutani T, Masui K, Poulou M, et al. Metabolic state of glioma stem cells and nontumorigenic cells. Proc

Natl Acad Sci U S A 2011;108:16062-7.

8. Ye XQ, Li Q, Wang GH, Sun FF, Huang GJ, Bian XW, et al. Mitochondrial and energy metabolism-related properties as novel indicators of lung cancer stem cells. Int J Cancer 2011;129:820-31.

9. Gurumurthy S, Xie SZ, Alagesan B, Kim J, Yusuf RZ, Saez B, et al. The Lkb1 metabolic sensor maintains haematopoietic stem cell survival. Nature 2010;468:659-63.

10. Lagadinou ED, Sach A, Callahan K, Rossi RM, Neering SJ, Minhajuddin M, et al. BCL-2 inhibition targets oxidative phosphorylation and selectively eradicates quiescent human leukemia stem cells. Cell Stem Cell 2013;12:329-41.

11. Nakada D, Saunders TL, Morrison SJ. Lkb1 regulates cell cycle and energy metabolism in haematopoietic stem cells. Nature 2010;468:653-8.

12. Sancho P, Barneda D, Heeschen C. Hallmarks of cancer stem cell metabolism. Br J Cancer 2016;114:1305-12.

13. Zong WX, Rabinowitz JD, White E. Mitochondria and Cancer. Mol Cell 2016;61:667-76.

14. Sabharwal SS, Schumacker PT. Mitochondrial ROS in cancer: initiators, amplifiers or an Achilles' heel? Nat Rev Cancer 2014;14:709-21.

15. Gorrini C, Harris IS, Mak TW. Modulation of oxidative stress as an anticancer strategy. Nat Rev Drug Discov 2013;12:931-47.

16. Panieri E, Santoro MM. ROS homeostasis and metabolism: a dangerous liason in cancer cells. Cell Death Dis 2016;7:e2253.

17. Chio IIC, Tuveson DA. ROS in Cancer: The Burning Question. Trends Mol Med 2017;23:411-29.

18. Ito K, Suda T. Metabolic requirements for the maintenance of self-renewing stem cells. Nat Rev Mol Cell Biol 2014;15:243-56.

19. Simsek T, Kocabas F, Zheng JK, DeBerardinis RJ, Mahmoud AI, Olson EN, et al. The Distinct Metabolic Profile of Hematopoietic Stem Cells Reflects Their Location in a Hypoxic Niche. Cell Stem Cell 2010;7:380-90.

20. Maryanovich M, Oberkovitz G, Niv H, Vorobiyov L, Zaltsman Y, Brenner O, et al. The ATM-BID pathway regulates quiescence and survival of haematopoietic stem cells. Nat Cell Biol 2012;14:535-41.

21. Maryanovich M, Gross A. A ROS rheostat for cell fate regulation. Trends Cell Biol 2013;23:129-34.

22. Cross CE, Halliwell B, Borish ET, Pryor WA, Ames BN, Saul RL, et al. Oxygen radicals and human disease. Ann Intern Med 1987;107:526-45.

23. Andersen JK. Oxidative stress in neurodegeneration: cause or consequence? Nat Med 2004;10 Suppl:S18-25.

24. Mugge A. The role of reactive oxygen species in atherosclerosis. Z Kardiol 1998;87:851-64.

25. Paravicini TM, Touyz RM. Redox signaling in hypertension.

Cardiovasc Res 2006;71:247-58.

26. Haigis MC, Yankner BA. The aging stress response. Mol Cell 2010;40:333-44.

27. Fridovich I. Superoxide anion radical (O2-.), superoxide dismutases, and related matters. J Biol Chem 1997;272:18515-7.

28. Murphy MP. How mitochondria produce reactive oxygen species. Biochem J 2009;417:1-13.

29. Schneider H, Lemasters JJ, Hackenbrock CR. Lateral diffusion of ubiquinone during electron transfer in phospholipid- and ubiquinone-enriched mitochondrial membranes. J Biol Chem 1982;257:10789-93.

30. Yano T, Dunham WR, Ohnishi T. Characterization of the delta muH+-sensitive ubisemiquinone species (SQ(Nf)) and the interaction with cluster N2: new insight into the energy-coupled electron transfer in complex I. Biochemistry 2005;44:1744-54.

31. Smith J, Ladi E, Mayer-Proschel M, Noble M. Redox state is a central modulator of the balance between self-renewal and differentiation in a dividing glial precursor cell. Proc Natl Acad Sci U S A 2000;97:10032-7.

32. Simsek T, Kocabas F, Zheng J, Deberardinis RJ, Mahmoud AI, Olson EN, et al. The distinct metabolic profile of hematopoietic stem cells reflects their location in a hypoxic niche. Cell Stem Cell 2010;7:380-90.

33. Suda T. Hematopoiesis and bone remodeling. Blood 2011;117:5556-7.

34. Tothova Z, Gilliland DG. FoxO transcription factors and stem cell homeostasis: insights from the hematopoietic system. Cell Stem Cell 2007;1:140-52.

35. Ito K, Hirao A, Arai F, Matsuoka S, Takubo K, Hamaguchi I, et al. Regulation of oxidative stress by ATM is required for self-renewal of haematopoietic stem cells. Nature 2004;431:997-1002.

36. Ito K, Hirao A, Arai F, Takubo K, Matsuoka S, Miyamoto K, et al. Reactive oxygen species act through p38 MAPK to limit the lifespan of hematopoietic stem cells. Nat Med 2006;12:446-51.

37. Tothova Z, Kollipara R, Huntly BJ, Lee BH, Castrillon DH, Cullen DE, et al. FoxOs are critical mediators of hematopoietic stem cell resistance to physiologic oxidative stress. Cell 2007;128:325-39.

38. Shackleton M, Vaillant F, Simpson KJ, Stingl J, Smyth GK, Asselin-Labat ML, et al. Generation of a functional mammary gland from a single stem cell. Nature 2006;439:84-8.

39. Stingl J, Eirew P, Ricketson I, Shackleton M, Vaillant F, Choi D, et al. Purification and unique properties of mammary epithelial stem cells. Nature 2006;439:993-7.

40. Cairns RA, Harris IS, Mak TW. Regulation of cancer cell metabolism. Nat Rev Cancer 2011;11:85-95.

41. Diehn M, Cho RW, Lobo NA, Kalisky T, Dorie MJ, Kulp AN, et al.

Association of reactive oxygen species levels and radioresistance in cancer stem cells. Nature 2009;458:780-3.

42. Kim HM, Haraguchi N, Ishii H, Ohkuma M, Okano M, Mimori K, et al. Increased CD13 expression reduces reactive oxygen species, promoting survival of liver cancer stem cells via an epithelial-mesenchymal transition-like phenomenon. Ann Surg Oncol 2012;19 Suppl 3:S539-48.

43. Song IS, Jeong YJ, Jeong SH, Heo HJ, Kim HK, Bae KB, et al. FOXM1-Induced PRX3 Regulates Stemness and Survival of Colon Cancer Cells via Maintenance of Mitochondrial Function. Gastroenterology 2015;149:1006-16 e9.

44. Lewis CA, Parker SJ, Fiske BP, McCloskey D, Gui DY, Green CR, et al. Tracing compartmentalized NADPH metabolism in the cytosol and mitochondria of mammalian cells. Mol Cell 2014;55:253-63.

45. Ciccarese F, Ciminale V. Escaping Death: Mitochondrial Redox Homeostasis in Cancer Cells. Front Oncol 2017;7:117.

46. Lee E, Yang J, Ku M, Kim NH, Park Y, Park CB, et al. Metabolic stress induces a Wnt-dependent cancer stem cell-like state transition. Cell Death Dis 2015;6:e1805.

47. <2016_Oncotarget_Integrated omics-analysis reveals Wnt mediated NAD metabolic reprogramming in cancer stem like cells.pdf>.

48. Park KC, Kim SW, Jeon JY, Jo AR, Choi HJ, Kim J, et al. Survival of Cancer Stem-Like Cells Under Metabolic Stress via CaMK2α-mediated

Upregulation of Sarco/Endoplasmic Reticulum Calcium ATPase Expression. Clinical Cancer Research 2018;24:1677-90.

49. Mailloux RJ, McBride SL, Harper ME. Unearthing the secrets of mitochondrial ROS and glutathione in bioenergetics. Trends Biochem Sci 2013;38:592-602.

50. Kuntz EM, Baquero P, Michie AM, Dunn K, Tardito S, Holyoake TL, et al. Targeting mitochondrial oxidative phosphorylation eradicates therapy-resistant chronic myeloid leukemia stem cells. Nat Med 2017;23:1234-40.

51. Viale A, Pettazzoni P, Lyssiotis CA, Ying H, Sanchez N, Marchesini M, et al. Oncogene ablation-resistant pancreatic cancer cells depend on mitochondrial function. Nature 2014;514:628-32.

52. Lee KM, Giltnane JM, Balko JM, Schwarz LJ, Guerrero-Zotano AL, Hutchinson KE, et al. MYC and MCL1 Cooperatively Promote Chemotherapy-Resistant Breast Cancer Stem Cells via Regulation of Mitochondrial Oxidative Phosphorylation. Cell Metab 2017;26:633-47 e7.

53. Roesch A, Vultur A, Bogeski I, Wang H, Zimmermann KM, Speicher D, et al. Overcoming intrinsic multidrug resistance in melanoma by blocking the mitochondrial respiratory chain of slow-cycling JARID1B(high) cells. Cancer Cell 2013;23:811-25.

54. Luo M, Shang L, Brooks MD, Jiagge E, Zhu Y, Buschhaus JM, et al.

Targeting Breast Cancer Stem Cell State Equilibrium through Modulation of Redox Signaling. Cell Metab 2018;28:69-86 e6.

55. Hirpara J, Eu JQ, Tan JKM, Wong AL, Clement MV, Kong LR, et al. Metabolic reprogramming of oncogene-addicted cancer cells to OXPHOS as a mechanism of drug resistance. Redox Biol 2019;25:101076.

56. Murphy MP, Holmgren A, Larsson NG, Halliwell B, Chang CJ, Kalyanaraman B, et al. Unraveling the biological roles of reactive oxygen species. Cell Metab 2011;13:361-6.

57. Yang H, Villani RM, Wang H, Simpson MJ, Roberts MS, Tang M, et al. The role of cellular reactive oxygen species in cancer chemotherapy. J Exp Clin Cancer Res 2018;37:266.

58. Park HJ, Carr JR, Wang Z, Nogueira V, Hay N, Tyner AL, et al. FoxM1, a critical regulator of oxidative stress during oncogenesis. The EMBO Journal 2009;28:2908-18.

59. Halasi M, Pandit B, Wang M, Nogueira V, Hay N, Gartel AL. Combination of oxidative stress and FOXM1 inhibitors induces apoptosis in cancer cells and inhibits xenograft tumor growth. Am J Pathol 2013;183:257-65.

60. Carr JR, Park HJ, Wang Z, Kiefer MM, Raychaudhuri P. FoxM1 mediates resistance to herceptin and paclitaxel. Cancer Res 2010;70:5054-63.

61. Khongkow P, Karunarathna U, Khongkow M, Gong C, Gomes AR, Yague E, et al. FOXM1 targets NBS1 to regulate DNA damage-induced senescence and epirubicin resistance. Oncogene 2014;33:4144-55.

62. Blacker TS, Mann ZF, Gale JE, Ziegler M, Bain AJ, Szabadkai G, et al. Separating NADH and NADPH fluorescence in live cells and tissues using FLIM. Nat Commun 2014;5:3936.

63. Pike LS, Smift AL, Croteau NJ, Ferrick DA, Wu M. Inhibition of fatty acid oxidation by etomoxir impairs NADPH production and increases reactive oxygen species resulting in ATP depletion and cell death in human glioblastoma cells. Biochimica et Biophysica Acta (BBA) - Bioenergetics 2011;1807:726-34.

64. Schafer ZT, Grassian AR, Song L, Jiang Z, Gerhart-Hines Z, Irie HY, et al. Antioxidant and oncogene rescue of metabolic defects caused by loss of matrix attachment. Nature 2009;461:109-13.

65. Jeon SM, Chandel NS, Hay N. AMPK regulates NADPH homeostasis to promote tumour cell survival during energy stress. Nature 2012;485:661-5.

66. Pavlova NN, Thompson CB. The Emerging Hallmarks of Cancer Metabolism. Cell Metab 2016;23:27-47.

67. Chandimali N, Jeong DK, Kwon T. Peroxiredoxin II Regulates Cancer Stem Cells and Stemness-Associated Properties of Cancers. Cancers

(Basel) 2018;10.

68. Sabharwal SS, Schumacker PT. Mitochondrial ROS in cancer: initiators, amplifiers or an Achilles' heel? Nature Reviews Cancer 2014;14:709-21.

69. Jo SH, Son MK, Koh HJ, Lee SM, Song IH, Kim YO, et al. Control of mitochondrial redox balance and cellular defense against oxidative damage by mitochondrial NADP+-dependent isocitrate dehydrogenase. J Biol Chem 2001;276:16168-76.

70. Kil IS, Kim SY, Lee SJ, Park JW. Small interfering RNA-mediated silencing of mitochondrial NADP+-dependent isocitrate dehydrogenase enhances the sensitivity of HeLa cells toward tumor necrosis factor-alpha and anticancer drugs. Free Radic Biol Med 2007;43:1197-207.

71. Kil IS, Chung KH, Park JW. Silencing of mitochondrial NADP+-dependent isocitrate dehydrogenase gene enhances selenite-induced apoptosis. Free Radic Res 2010;44:332-9.

72. Nilsson R, Jain M, Madhusudhan N, Sheppard NG, Strittmatter L, Kampf C, et al. Metabolic enzyme expression highlights a key role for MTHFD2 and the mitochondrial folate pathway in cancer. Nat Commun 2014;5:3128.

73. Fan J, Ye J, Kamphorst JJ, Shlomi T, Thompson CB, Rabinowitz JD. Quantitative flux analysis reveals folate-dependent NADPH production.

Nature 2014;510:298-302.

74. Nishimura T, Nakata A, Chen X, Nishi K, Meguro-Horike M, Sasaki S, et al. Cancer stem-like properties and gefitinib resistance are dependent on purine synthetic metabolism mediated by the mitochondrial enzyme MTHFD2. Oncogene 2019;38:2464-81.

ABSTRACT(IN KOREAN)

위암줄기세포에서 치료 표적으로서 미토콘드리아 활성산소 항상성 조절 기전

< 지도교수 정재호 >

연세대학교 대학원 의과학과

최혜지

암 줄기세포는 일반 암 세포와는 달리 스스로 재생하고 다른 세포로 분화 할 수 있는 무제한 재생능력을 가져 전이의 주요 원인으로 작용하며 높은 약물 저항성을 나타낸다. 특히 일부 환자들은 이런 암 줄기세포가 활성화 되면서 항암제 치료가 듣지 않는 '강한 저항성'을 보이기도 한다. 기존 항암요법으로는 치료할 수 없는 난치성 암이 이 경우에 해당된다.

최근 암 줄기세포는 미토콘드리아 기능이 일반 암 세포보다 향상되어 Glycolysis 보다 OXPHOS에 의존해 ATP를 생성하는 것이 다양한 암종에서 공통적으로 보고된 바 있다. 그러나 암 줄기세포를 타겟하는 정확한 메커니즘에 대해서는 잘 알려져 있지 않다. 본

연구에서는 미토콘드리아 활성 산소 항상성의 조절 기전을 규명함으로써, 암 줄기 세포에서 임상적으로 가장 큰 문제점인 약물 저항성을 타겟 할 있는 메커니즘적 근거를 제시하고자 한다.

암 줄기세포에서 미토콘드리아 기능이 향상되어 있음에도 불구하고 활성 산소가 낮게 유지되는 것을 확인 할 수 있었다. 항산화 효소 중 미토콘도리아에 존재하는 Prx3의 발현이 암 줄기 세포에서 높은 것을 확인하였으며, 전사 인자인 FoxM1에 의해 Prx3 발현이 조절 됨을 확인하였다. 또한 암 줄기세포는 지방산 산화를 통한 에너지 대사 과정에서 미토콘드리아에 존재하는 IDH2와 MTHFD2에 의존적으로 NADPH를 재생성 함으로써 활성 산소 항상성을 유지함을 확인 할 수 있었다.

본 연구는 표준 항암치료에 저항성이 있는 암 줄기세포의 잠재적 생존 원리를 규명했으며, 미토콘드리아 활성산소 항상성 유지 메커니즘을 표적으로 난치성 악성 암을 치료할 수 있는 실험적 근거를 제시하였다.

핵심되는 말 : oxidative phosphorylation; reactive oxygen species; cancer stem-like cell; FoxM1; fatty acid oxidation